

# **Synergy in energy transfer between ligand and Eu<sup>III</sup> ion in molecular Europium complex: a single-component white light emissive luminogens**

Rachna Devi, Kasturi Singh and Sivakumar Vaidyanathan

Department of Chemistry, National Institute of Technology Rourkela,

Rourkela-769 008, Odisha, India.

## **Table of contents**

General information synthesis.....	S2
NMR Spectra .....	S7
Fourier transform-Infrared spectroscopy (FT-IR).....	S11
UV and PL spectra .....	S13
Judd-Ofelt (J –O) analysis:.....	S9
Electrochemical Properties.....	S18
Phosphorescence study at 77K.....	S21
Thermal Study.....	S22
DFT analysis .....	S23
References .....	S23

**General Information for synthesis:** All the reaction was done in the inert atmosphere. Solvent THF is dried and distilled by using Na metal. All the commercially available reagents (Sigma Aldrich and Alpha aesar) were used without further refinement unless otherwise needed. The progress of all the reactions was checked by thin-layer chromatography (TLC) with silica gel 60 F254 Aluminium plates (Merck) at a regular interval of time. For the purification of crud reaction mass was carried out by the column chromatography using silica gel (Sigma-Aldrich).

**Measurements:** For recording the  $^1\text{H}$  and  $^{13}\text{C}$ -NMR spectra the AV 400 Advance-III 400MHz Fourier transform nuclear magnetic resonance (FT-NMR) Spectrometer Bruker Biospin International, Switzerland was used. All the  $^1\text{H}$  and  $^{13}\text{C}$ -NMR spectra were recorded in deuterated chloroform/dimethyl sulfoxide solution and tetramethylsilane (TMS) was used as a standard reference for chemical shift measurement. The Fourier transform infrared (FT-IR) spectra were recorded on a PerkinElmer, USA/RX-I FTIR, spectrophotometer, and elemental analysis was measured by an Elementar Analysen Systeme, Germany/Vario EL spectrometer. The PL emission and excitation spectra in the solution and solid were recorded by using the Edinburg spectrofluorometer FS- 5 instruments associated with SC – 10 modules and SC – 5 modules respectively. The photoluminescence quantum yield were recorded with horiba Jobin Yvon, HR 320 and the fluorescence quantum yield was measured with Edinburgh Instruments, spectrofluorometer, FS5, Integrating Sphere SC-30. The CIE color coordinate for all emission spectra is calculated by MATLAB software. The absorption spectra of all the synthesized compounds in solution form were utilizing UV-Visible spectrometer (Shimadzu Corporation, Japan or UV-2450 Perkin Elmer, USA/Lamda 25 and Lamda Perkin Elmer). The electrochemical properties of the ligands and their respective complex were estimated by utilizing cyclic voltammetry (CV), AUTOLAB 302N Modular potentiostat at RT in Dimethylformamide (DMF). The CV analysis is the set-up of mainly

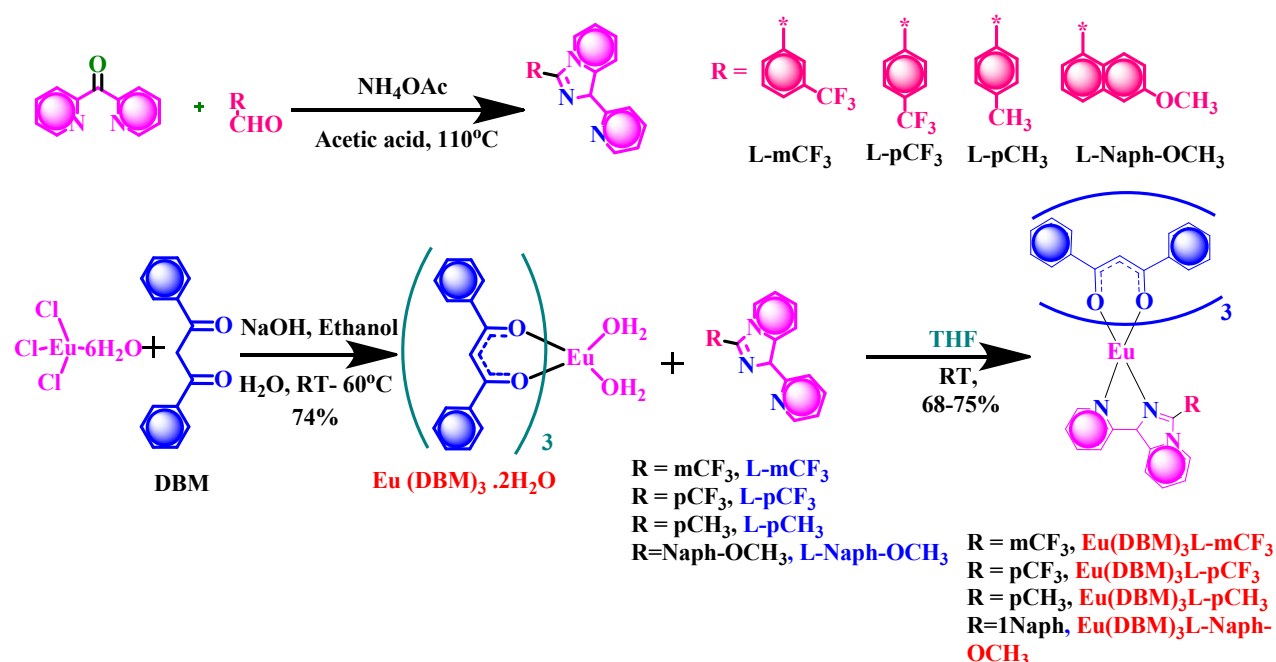
three electrode, the working (glass-carbon rod), auxiliary (counter, Pt wire) and reference (Ag/AgCl wire) electrodes. Dimethylformamide (DMF) containing 0.1 M  $\text{Bu}_4\text{NClO}_4$  was used as an electrolyte and the sweep rate was kept as  $100 \text{ mV s}^{-1}$ . The ligand sub-atomic structures were optimized within density functional theory (DFT) frame work utilizing B3LYP/6-31G (d, p) level of theory.

A UV-visible spectrum of the molecule is obtained by exciting molecule vertically after conformation of ground state geometry for the ligand. Further, to the depiction of PL emission and excitation mechanism of the Eu(III) complex, triplet energized condition of the ligand is additionally accesses by utilizing the same procedure specified previously. The optimization study of ligand is effectively accomplished by the G09W program. The Lifetime of the Eu(III) complex, as well as the ligand, were measured at 298 K with Edinburgh Instruments FLS 980 based on the time-correlated single photon counting technology upon the excitation at 380 nm. A pulsed xenon lamp was used as the excitation source, and the signals were detected with a photomultiplier. All the measurements were carried out at room temperature (RT).

### **Materials:**

The synthesis of Eu(III) chloride ( $\text{EuCl}_3 \cdot 6\text{H}_2\text{O}$ ) from Eu(III) oxide is done by the well-known process.<sup>1</sup>The resultant product ( $\text{EuCl}_3 \cdot 6\text{H}_2\text{O}$ ) was then treated with an alcoholic solution of DBM (3 eq.) in the presence of 1 N sodium hydroxide solution (3.1 eq.) to get  $\text{Eu}(\text{DBM})_3(\text{H}_2\text{O})_2$  (NMR spectra are shown in the Fig.S9). 1, 10-Phenanthroline-5, 6-dione was synthesized from 1, 10-phenanthroline by a previously reported procedure.<sup>2-3</sup> All the ligands were successfully synthesized by a well-reported procedure.<sup>4-5</sup>

## General synthesis of ligand and Eu(III) complexes:



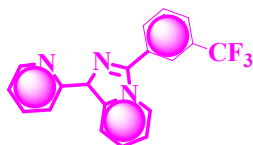
**Scheme S1.** The synthesis route of the ligands and corresponding Eu(III) complexes.

## General Synthesis of Ligand:

2,2'-Dipyridyl ketone (0.5 g, 2.717 mmol) was taken in a round-bottom flask, and to this was added glacial acetic acid (15 mL) at room temperature (RT). To this reaction mixture were subsequently added the aldehyde compound (3-(Trifluoromethyl) benzaldehyde/ 4-(Trifluoromethyl) Benzaldehyde/ p-Tolulenealdehyde/ 6-methoxy-2-naphthaldehyde) (0.946 g, 5.434 mmol) and ammonium acetate (1.04 g, 13.58 mmol). Then, the resultant mixture was stirred for 12 h at 110 °C. The progress of the reaction was monitored by TLC (MeOH in chloroform 1:9, R<sub>f</sub> - 0.3). The reaction mixture was poured into a minimum amount of water and then ammonium hydroxide (NH<sub>4</sub>OH) solution was added to neutralize the reaction mixture (pH = 7.0). The obtained solid was filtered and dissolved in dichloromethane, followed by dried with anhydrous sodium sulphate. The solvent was evaporated to get of crude compound (0.710 g). This was purified with column chromatography by using silica gel (100–200 mesh), eluent with 5% methanol in chloroform. The obtained product was

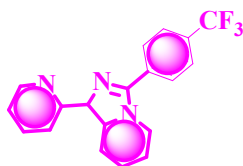
dissolved in a minimum amount of THF solution and an excess amount of hexane was added to the same; the pale yellow color solid that was formed is 450 mg (50.0%). The NMR spectra are displayed in Fig.S1–S8 and mass spectra are displayed in the Fig.S9-16.

**1-(pyridin-2-yl)-3-(3-(trifluoromethyl)phenyl)-1,8a-dihydroimidazo[1,5-a]pyridine (L-mCF<sub>3</sub>):**



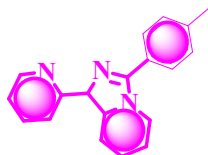
**<sup>1</sup>H-NMR (400 MHz, CDCl<sub>3</sub>, TMS, δ ppm):** 8.77(d, *J*=8, 1H), 8.76-8.67(m, 1H), 8.27(dd, *J*=0.8, 2H), 8.17(s, 1H), 8.08(d, *J*=7.2, 1H), 7.78-7.68(m, 3H), 7.17-7.13(m, 1H), 7.03-6.98(m, 1H), 6.78-6.74(m, 1H) **<sup>13</sup>C-NMR (100 MHz, CDCl<sub>3</sub>, TMS, δ ppm):** 148.81, 131.28, 130.98, 129.62, 125.22, 122.04, 121.22, 120.78, 120.13, 114.68, 77.34, 77.23, 77.03, 76.71, Calculated m/z ratio = 341.11 found m/z ratio = 340.05

**1-(pyridin-2-yl)-3-(4-(trifluoromethyl)phenyl)-1,8a-dihydroimidazo[1,5-a]pyridine (L-pCF<sub>3</sub>):**



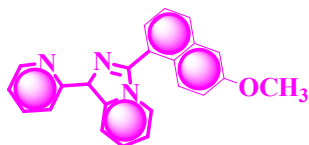
**<sup>1</sup>H-NMR (400 MHz, CDCl<sub>3</sub>, TMS, δ ppm):** δ 8.78(d, *J*=9.2Hz, 1H), 8.66(dd, *J*=5.2Hz, 1H), 8.29(dd, *J*=7.6Hz, 2H), 8.03(d, *J*=8Hz, 2H), 7.83(d, *J*=8Hz, 2H), 7.78- 7.44(m, 1H), 7.171-7.00(m, 1H), 6.87(t, *J*=1.2, 1H), 6.75( t, *J*=1.2, 1H). **<sup>13</sup>C-NMR (100 MHz, CDCl<sub>3</sub>, TMS, δ ppm):** 136.37, 128.35, 126.03, 122.11, 121.51, 121.31, 120.78, 114.63, 77.34, 77.02, 76.70 Calculated m/z ratio = 341.11 found m/z = 340.15

**7-methyl-1-(pyridin-2-yl)-3-(p-tolyl)-1,7,8,8a-tetrahydroimidazo[1,5-a]pyridine (L-pCH<sub>3</sub>):**



**<sup>1</sup>H-NMR (400 MHz, CDCl<sub>3</sub>, TMS, δ ppm):** 8.71(d, *J*=9.2,1H), 8.65-8.64(m,1H),8.27-8.25(m,2H), 7.73(dd, *J*=8,2, 3H), 7.38(d,*J*=8, 2H), 7.12-7.09(m,1H), 6.95-6.92(m, 1H), 6.68-6.64(m,1H), 2.47(s,3H)  
**<sup>13</sup>C-NMR (100 MHz, CDCl<sub>3</sub>, TMS, δ ppm):** 148.84, 139.03, 138.33, 136.39, 130.13, 129.75, 128.34, 127.17, 121.76, 121.73, 121.04, 120.41, 120.04, 113.81, 77.35, 77.03, 76.71  
 Calculated m/z ratio = 303.17 found m/z = 302.89

**3-(6-methoxynaphthalen-1-yl)-1-(pyridin-2-yl)-1,8a-dihydroimidazo[1,5-a]pyridine (L-Naph-OCH<sub>3</sub>):**



**<sup>1</sup>H-NMR (400 MHz, CDCl<sub>3</sub>, TMS, δ ppm):** δ 8.74 (d, *J*=8.8,1H), 8.66(d,*J*=4.8,1H),8.37(d,*J*=7.2,1H),8.30(d,*J*=8,2H),7.95(t,*J*=8.8,2H), 7.85(d,*J*=8.8,1H),7.77-7.73(m,1H), 7.25-7.23(m,2H), 7.14-7.12(m,1H), 6.99-6.95(m,1H), 6.72-6.68(m,1H),3.99(s,3H)  
**<sup>13</sup>C-NMR (100 MHz, CDCl<sub>3</sub>, TMS, δ ppm):** 158.40, 155.08, 149.01, 136.28, 134.63, 129.82, 128.83, 127.65, 127.37, 126.45, 125.24, 121.87, 121.87, 121.73, 121.08, 120.45, 119.98, 119.60, 113.96, 105.8, 77.34, 77.02, 76.70, 55.40, 30.95, Calculated m/z = 353.15 found m/z ratio = 352.21

**Eu(DBM)<sub>3</sub>L-mCF<sub>3</sub>**; The solution of Eu(DBM)<sub>3</sub>(H<sub>2</sub>O)<sub>2</sub> (0.150 g, 0.175mmol) in dry THF (15 mL) was taken in round bottom flask and stirrer constantly unless a clear solution obtain, after 20 minutes a mixture of L-mCF<sub>3</sub>(0.0810g, 0.174) in dry THF was added slowly drop by drop. The reaction mixture was then stirred for 6 hours at 60°C in inert condition.<sup>6</sup> The completion of the reaction is monitored by TLC then the mixture was concentrated and then dissolved in the minimum amount of THF. To this solution, excess hexane was added by the wall of the round bottom flask; the precipitate was obtained. The reaction mixture was filter

and washed several time to achieve the final complex in powder (pale yellow color solid with 110 mg (~73.4%)) form. **ESI-MS:**  $m/z = 1290.16$ , found:  $m/z = 1290.85$   $[M + H]^+$ .

**Elemental analysis:** Anal. Calc. for  $C_{64}H_{46}EuF_3N_3O_6$ : C, 66.15; H, 3.99; N, 3.62. Found: C, 65.95; H, 3.54; N, 3.44%.

**Eu(DBM)<sub>3</sub>L-pCF<sub>3</sub>**; The complex was synthesized by previously described procedure using **L-pCF<sub>3</sub>** as the ligand instead of L-mCF<sub>3</sub>. **ESI-MS:**  $m/z = 1290.16$ , found:  $m/z = 1314.10$   $[M + Na]^+$ . Elemental analysis: Anal. Calc. for  $C_{64}H_{46}EuF_3N_3O_6$ : C, 66.15; H, 3.99; N, 3.62. Found: C, 65.77; H, 3.43; N, 3.31%.

**Eu(DBM)<sub>3</sub>L-pCH<sub>3</sub>**; The complex was synthesized by previously described procedure using **L-pCH<sub>3</sub>** as the ligand instead of L-mCF<sub>3</sub>. **ESI-MS:**  $m/z = 1236.19$ , found:  $m/z = 1237.32$   $[M + H]^+$ . Elemental analysis: Anal. Calc. for  $C_{64}H_{49}EuF_3N_3O_6$ : C, 69.37; H, 4.46; N, 3.79. Found: C, 69.15; H, 4.36; N, 3.43%.

**Eu(DBM)<sub>3</sub>L-Naph-OCH<sub>3</sub>**; The complex was synthesized by previously described procedure using **L-Naph-OCH<sub>3</sub>** as the ligand instead of L-mCF<sub>3</sub>. **ESI-MS:**  $m/z = 1272.31$ , found:  $m/z = 1294.32$   $[M + Na]^+$ . Anal. Calc. for  $C_{68}H_{51}EuN_3O_6$ : C, 69.56; H, 4.38; N, 3.58. Found: C, 69.43; H, 4.17; N, 3.32%.

## NMR Spectroscopy:

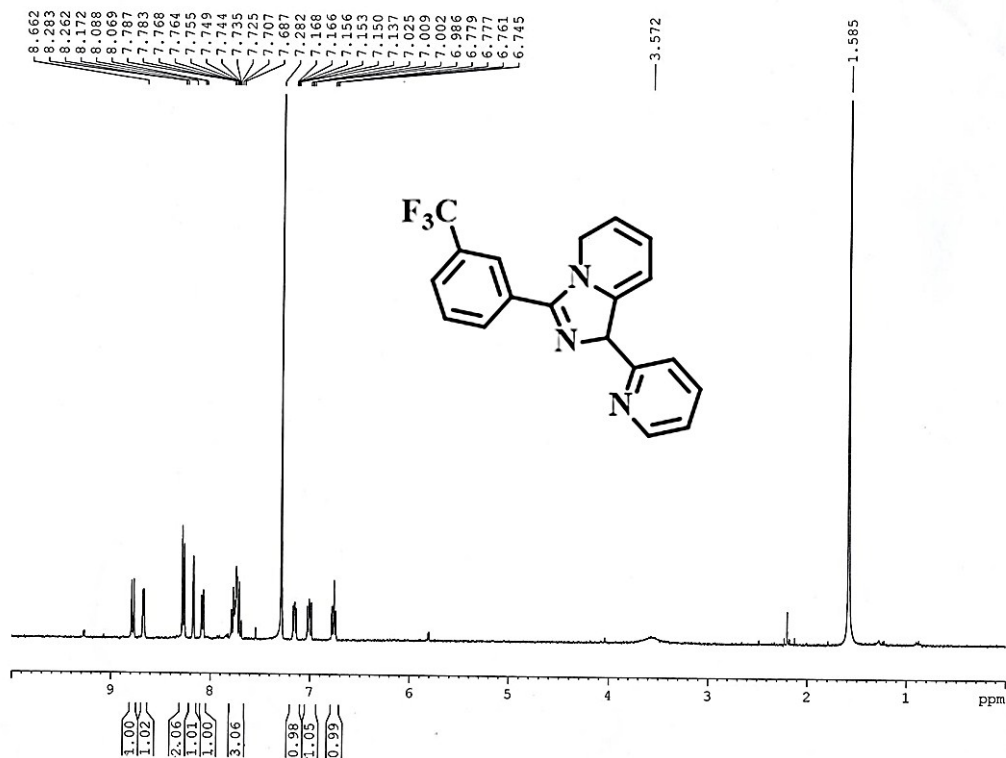


**Fig. S1** <sup>1</sup>H NMR spectroscopy of L-mCF<sub>3</sub> in CDCl<sub>3</sub>

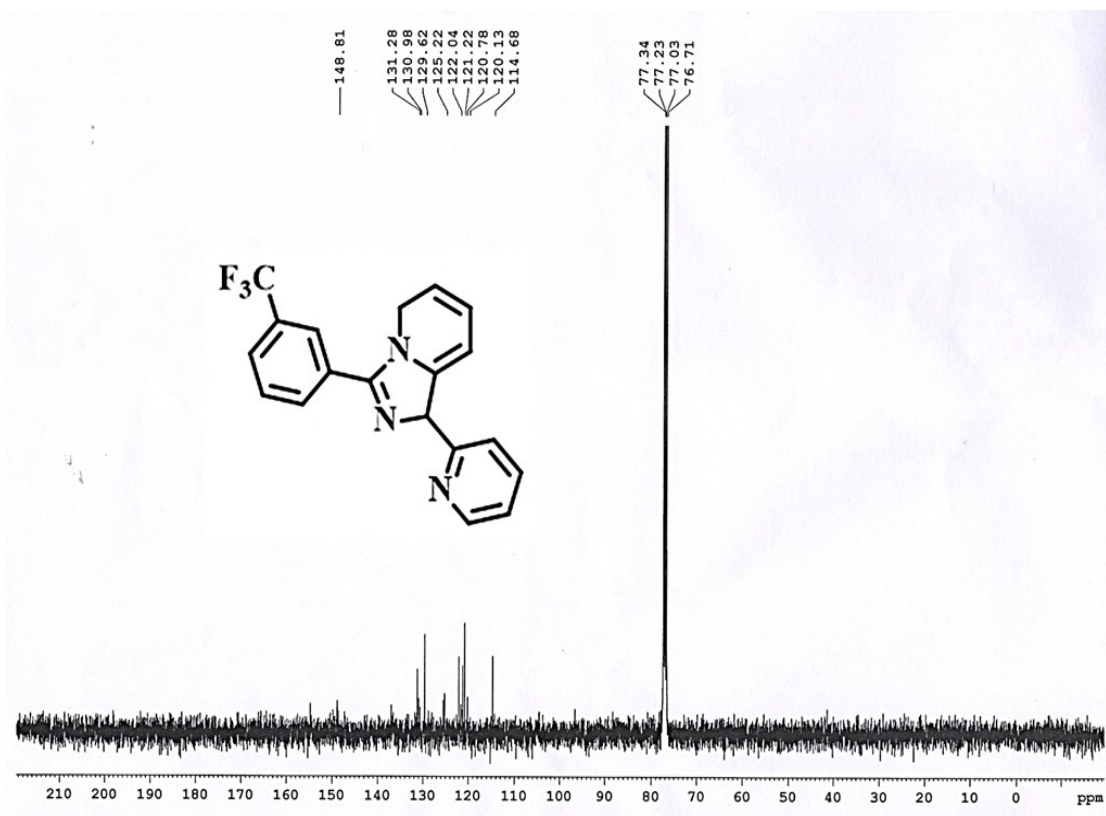


**Fig. S2** <sup>13</sup>C NMR spectroscopy of L-mCF<sub>3</sub> in CDCl<sub>3</sub>



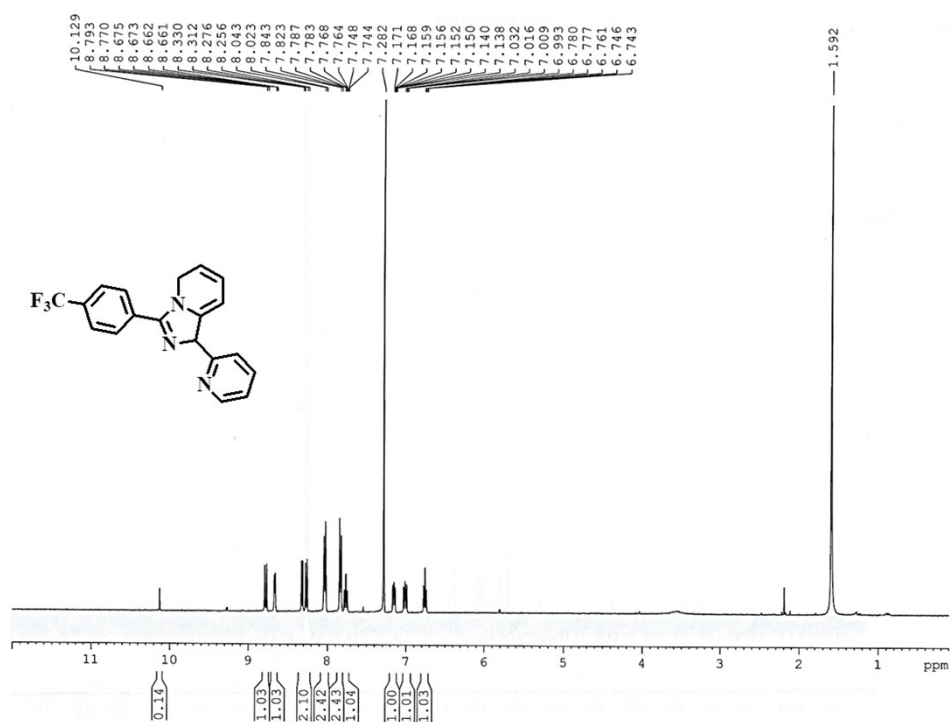


**Fig. S3** <sup>1</sup>H NMR spectroscopy of L-pCF<sub>3</sub> in CDCl<sub>3</sub>

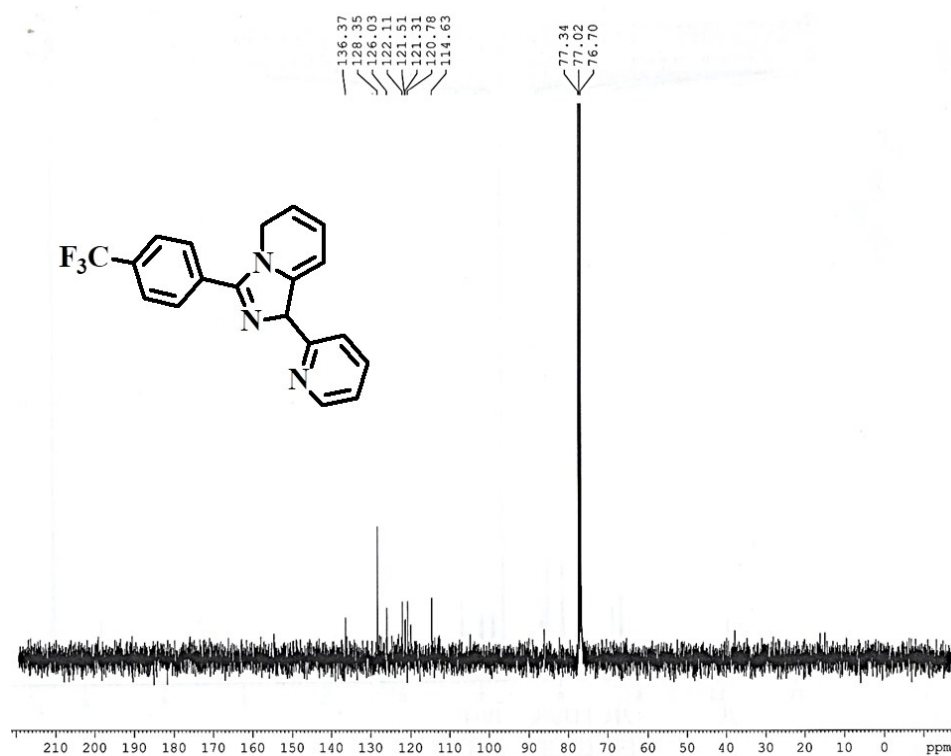


**Fig. S4** <sup>13</sup>C NMR spectroscopy of L-pCH<sub>3</sub> in CDCl<sub>3</sub>

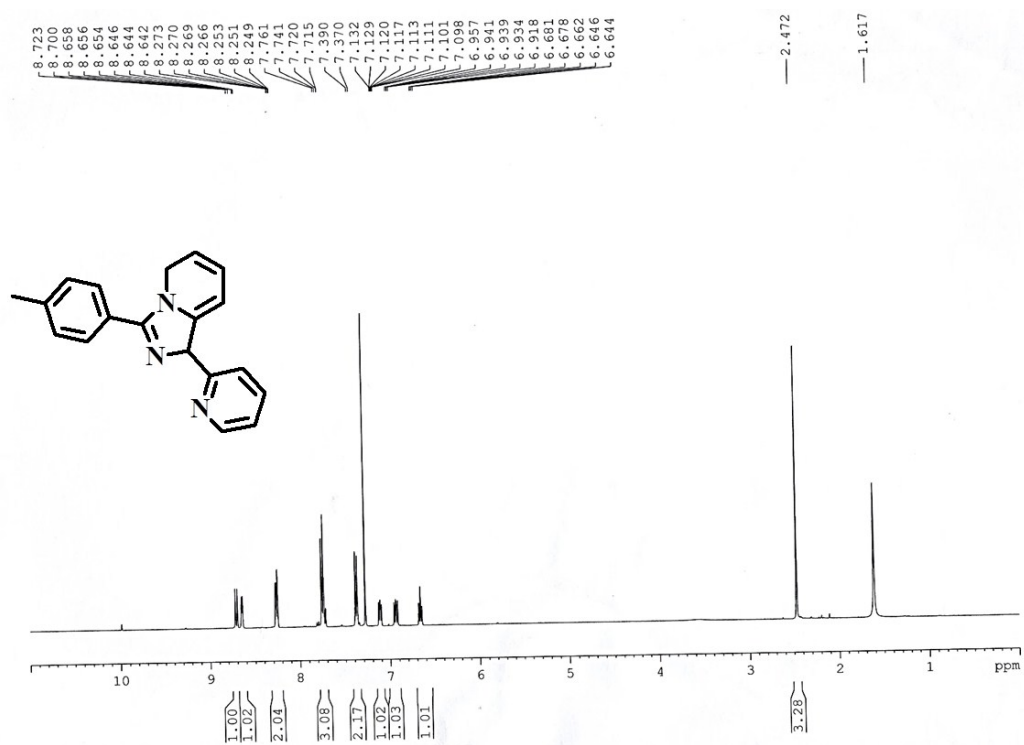


Fig. S5 <sup>1</sup>H NMR spectroscopy of L-pCH<sub>3</sub> in CDCl<sub>3</sub>

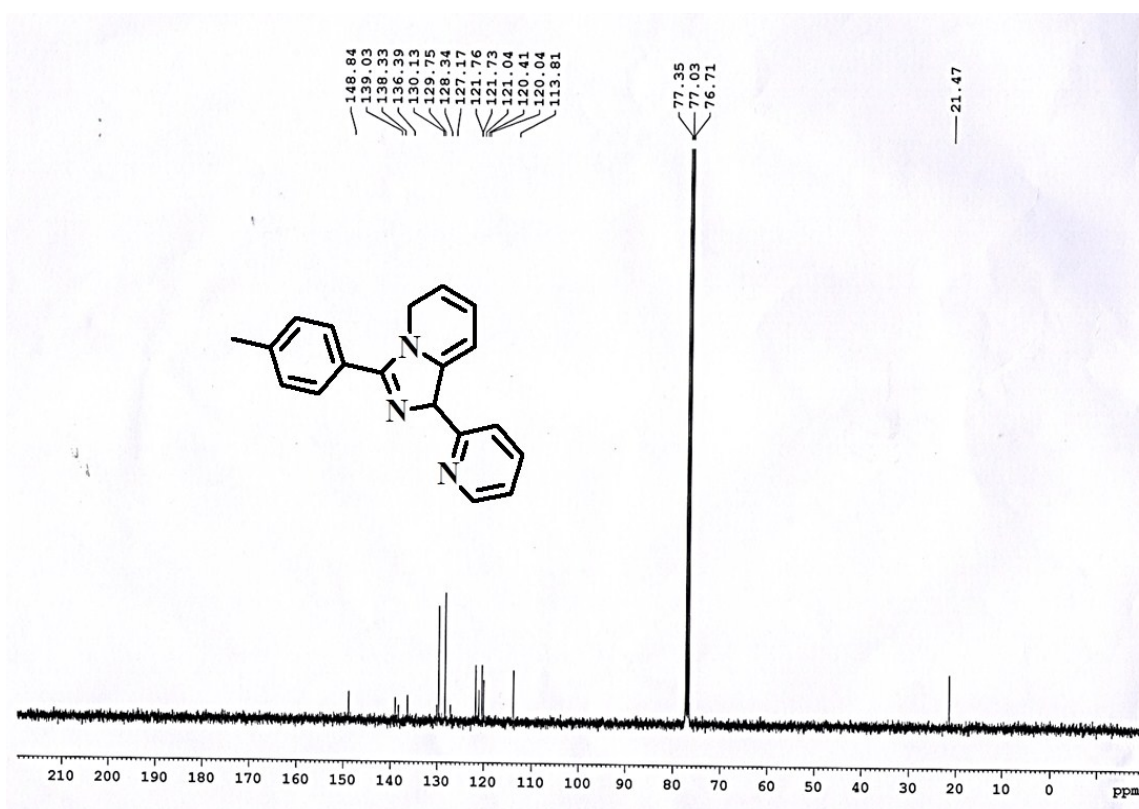
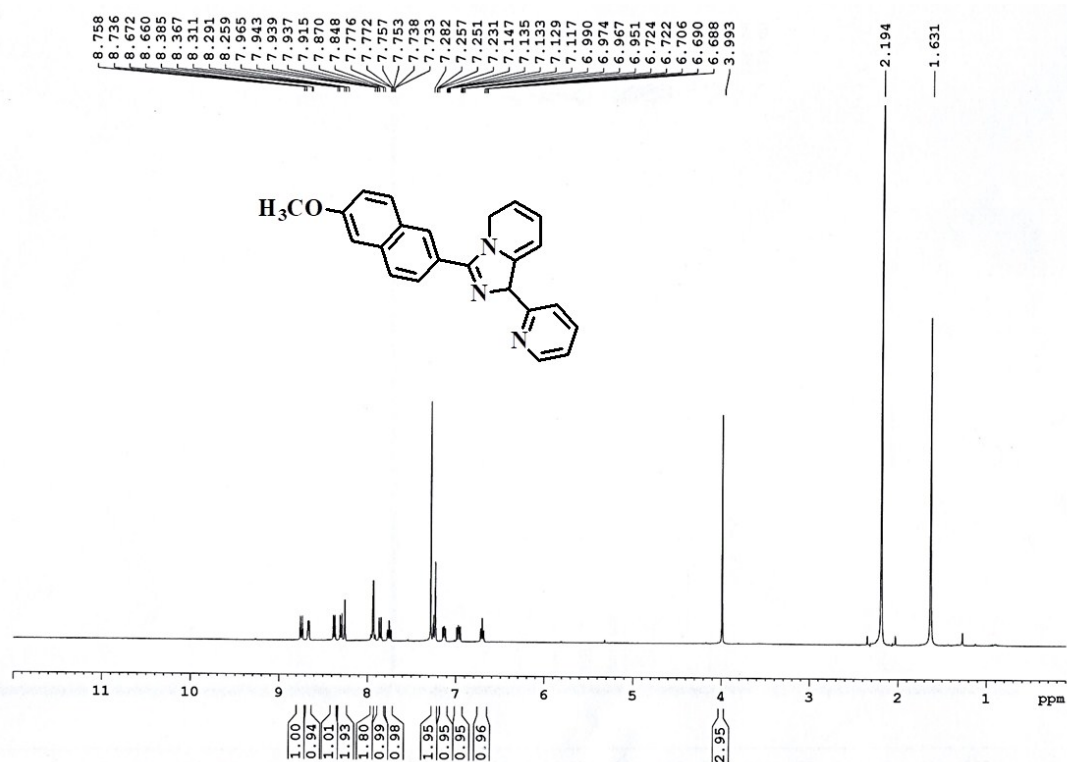
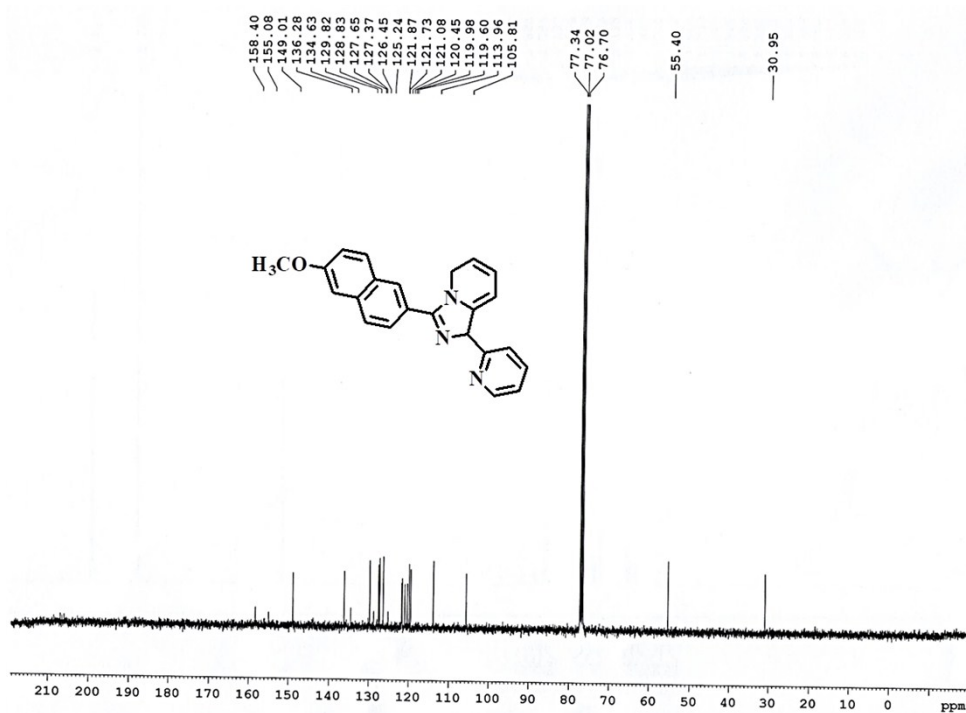


Fig. S6 <sup>13</sup>C NMR spectroscopy of L-pCH<sub>3</sub> in CDCl<sub>3</sub>



**Fig. S7** <sup>1</sup>H NMR spectroscopy of L-Naph-OCH<sub>3</sub> in CDCl<sub>3</sub>



**Fig. S8** <sup>13</sup>C NMR spectroscopy of L-Naph-OCH<sub>3</sub> in CDCl<sub>3</sub>

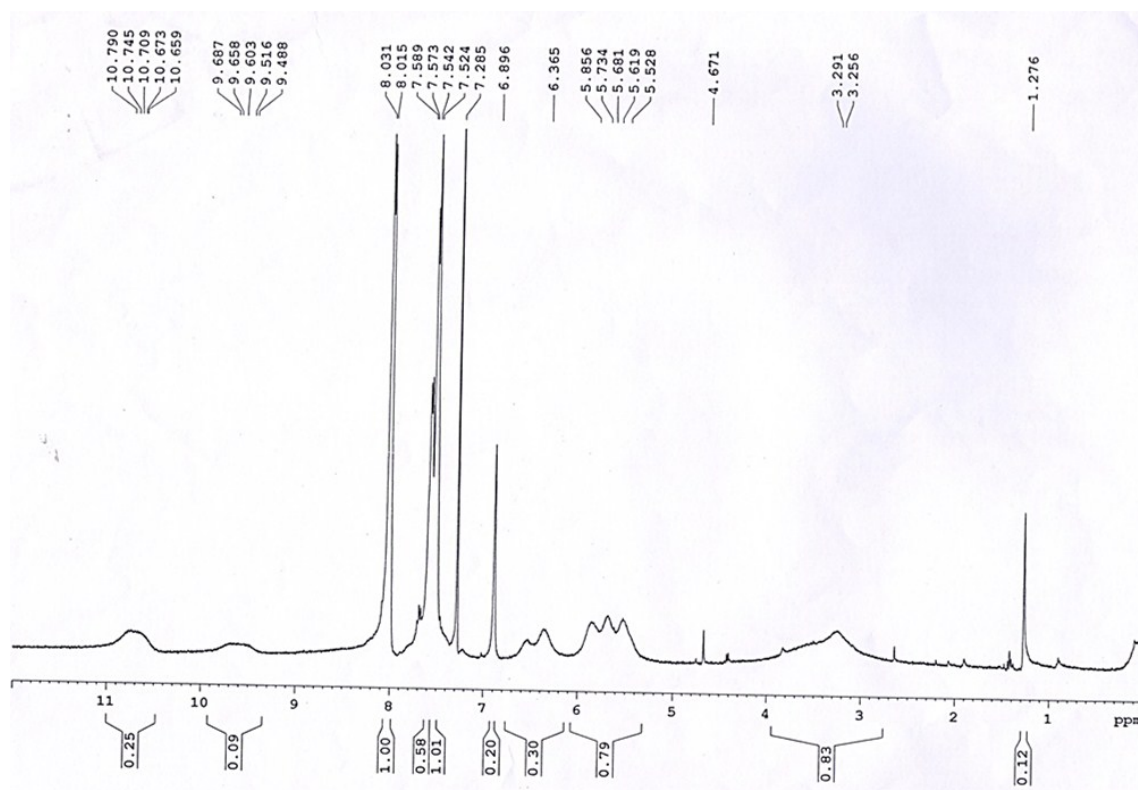


**Fig. S9**  $^1\text{H}$ - NMR spectroscopy of  $\text{Eu}(\text{DBM})_3 \cdot 2\text{H}_2\text{O}$  in  $\text{CDCl}_3$

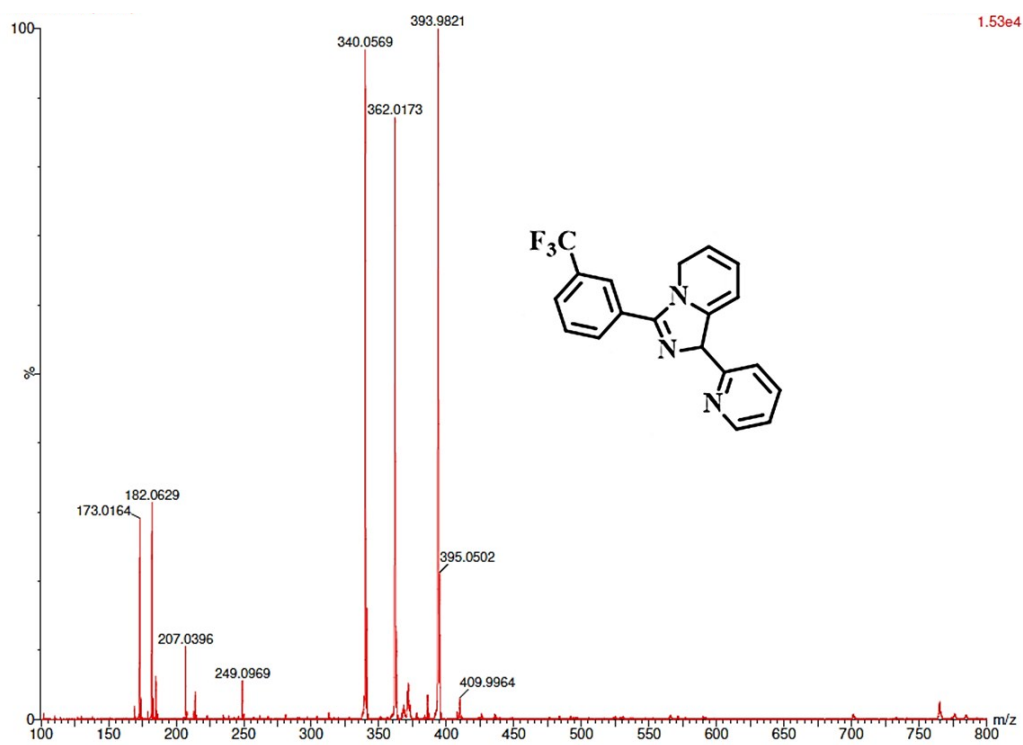


**Fig. S10** Mass spectra of L-mCF<sub>3</sub>

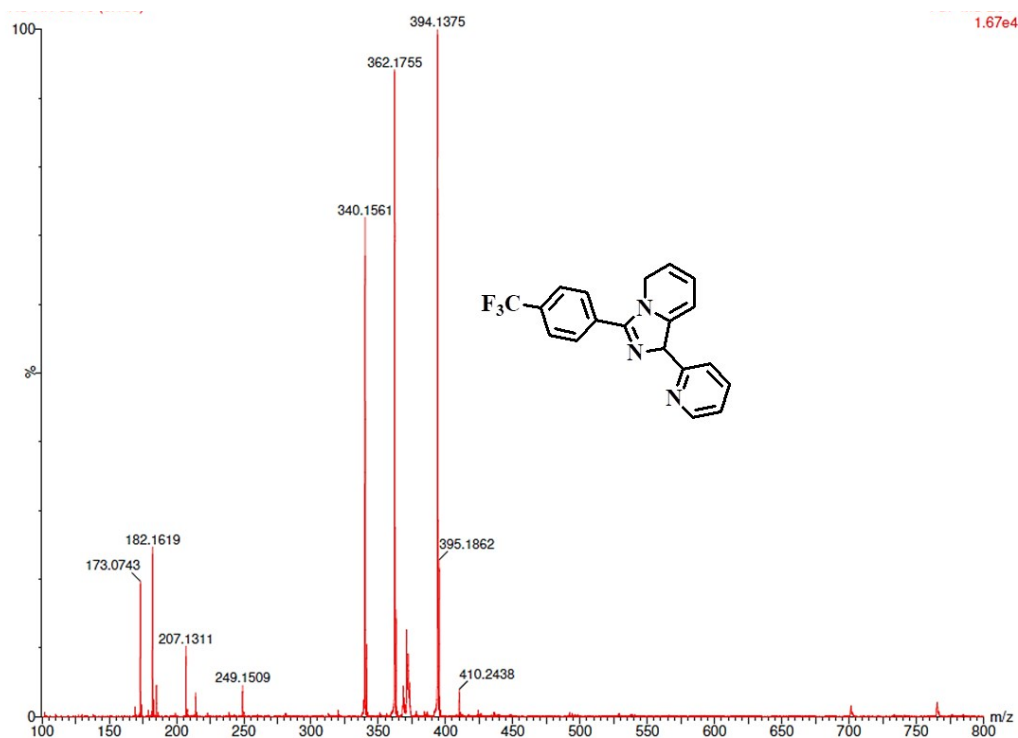


**Fig. S11** Mass spectra of L-pCF<sub>3</sub>

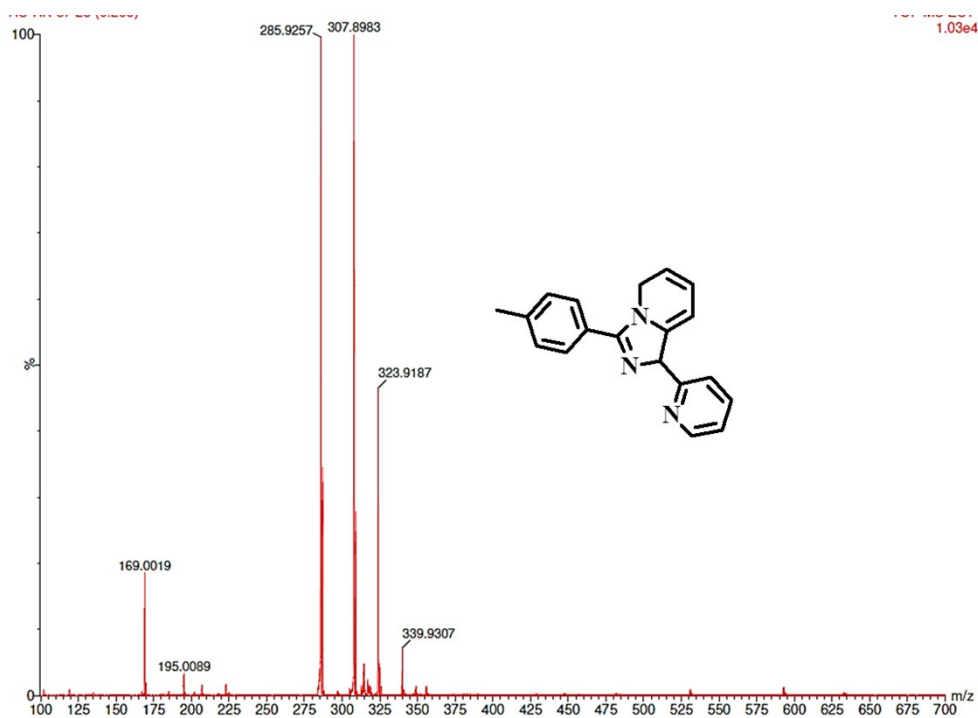


**Fig. S12** Mass spectra of L-pCH<sub>3</sub>

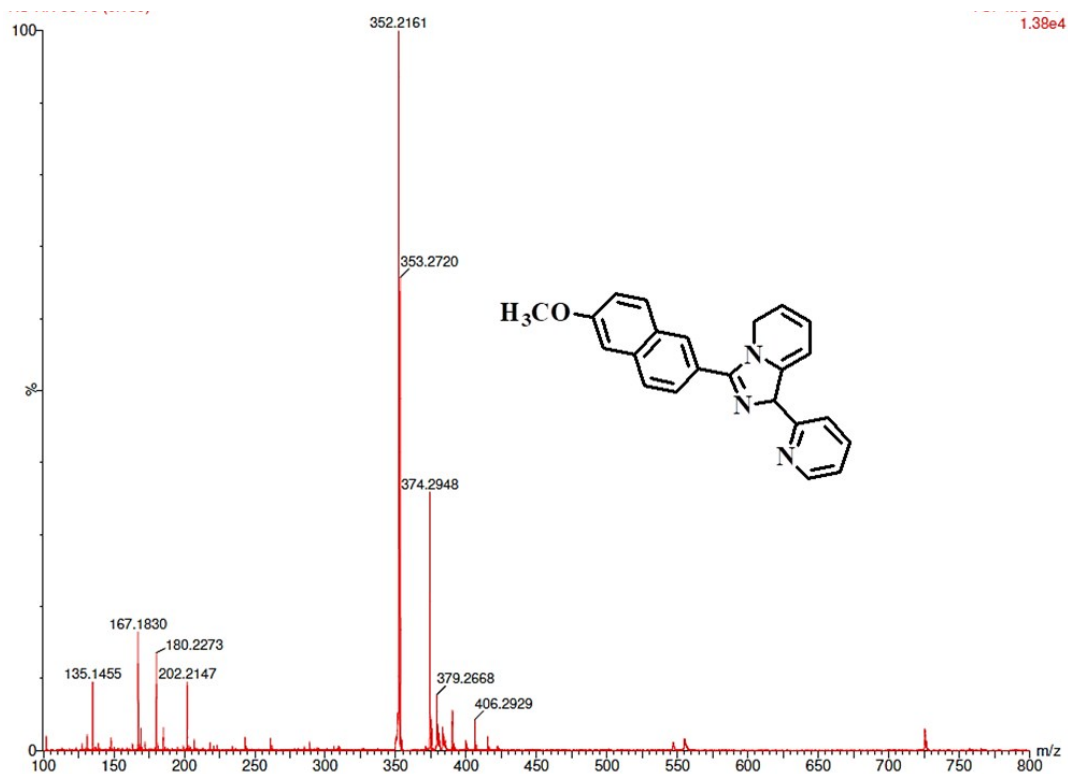


**Fig. S13** Mass spectra of L-Naph-OCH<sub>3</sub>

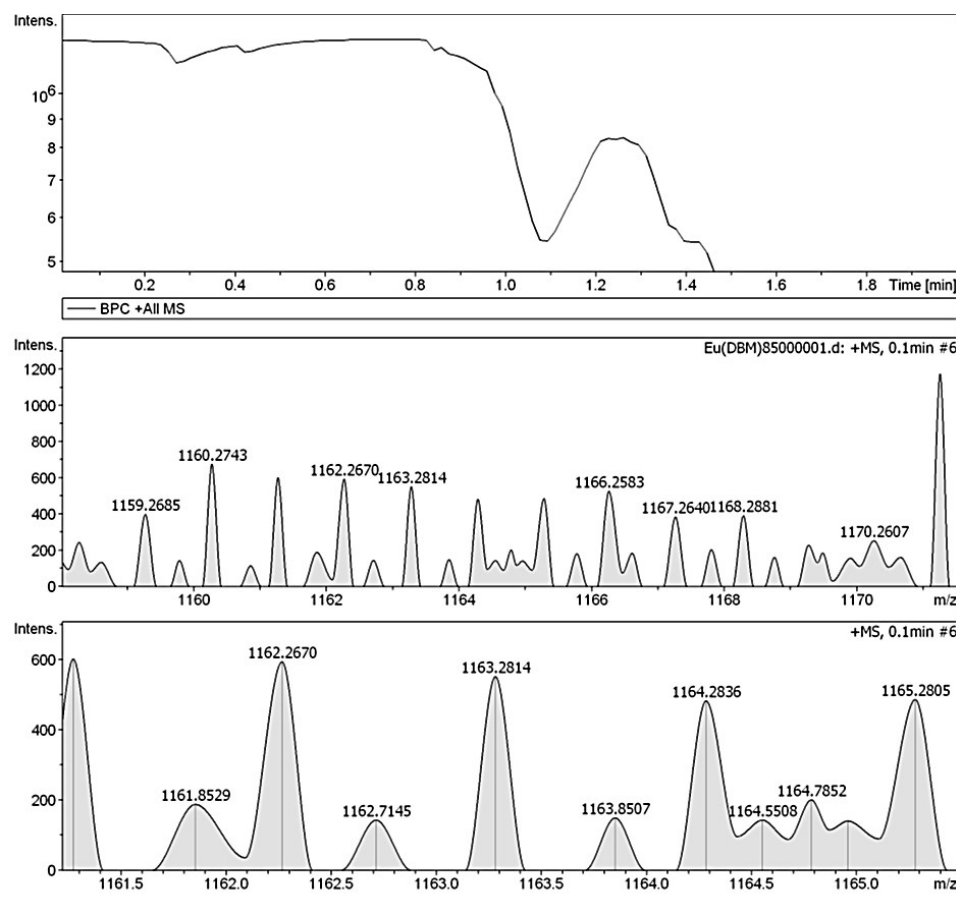


**Fig. S14** Mass spectra of  $\text{Eu}(\text{DDBM})_3\text{L-mCF}_3$  in  $\text{CDCl}_3$

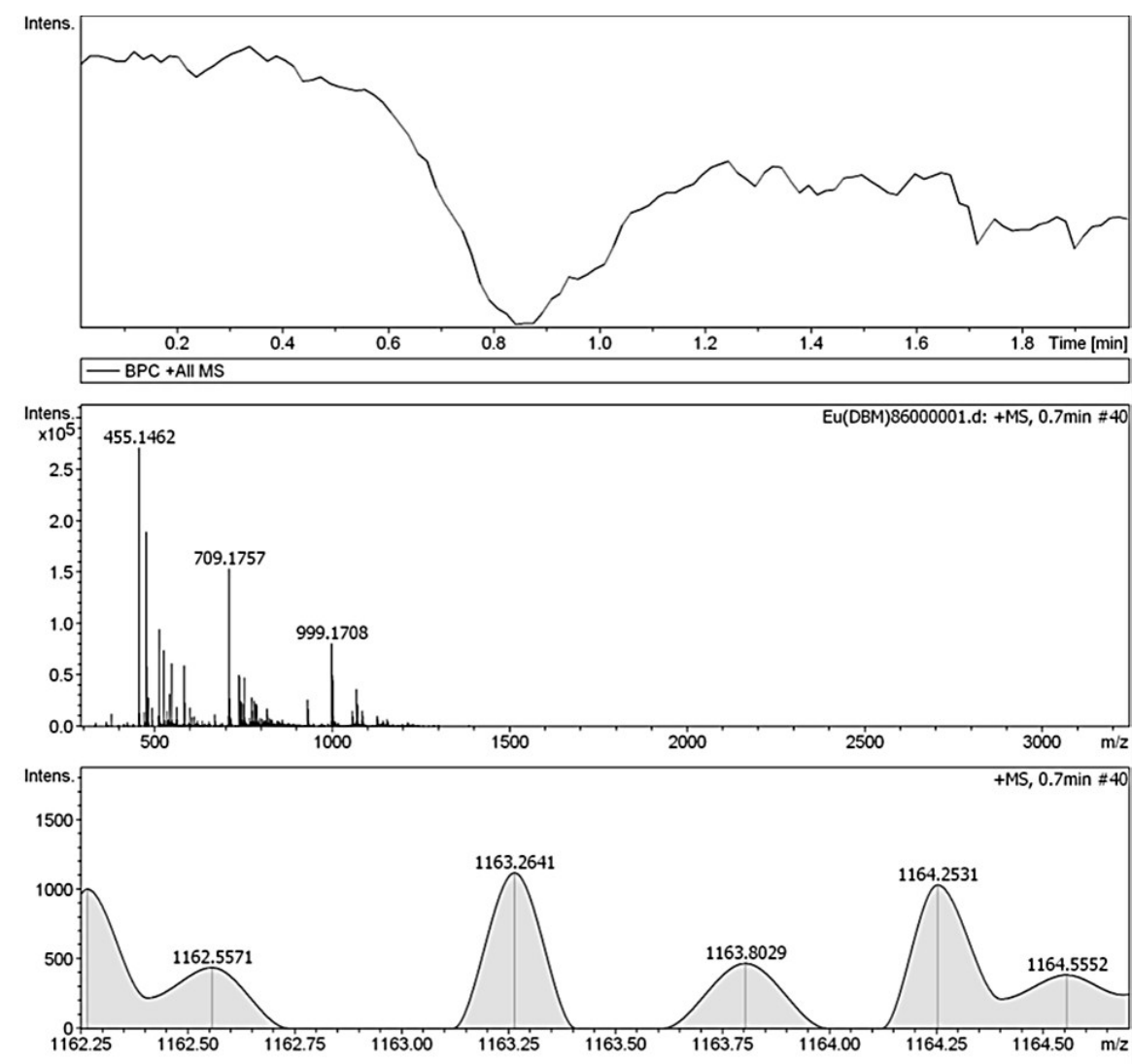


**Fig. S15** Mass spectra of  $\text{Eu}(\text{DDBM})_3\text{L-pCF}_3$

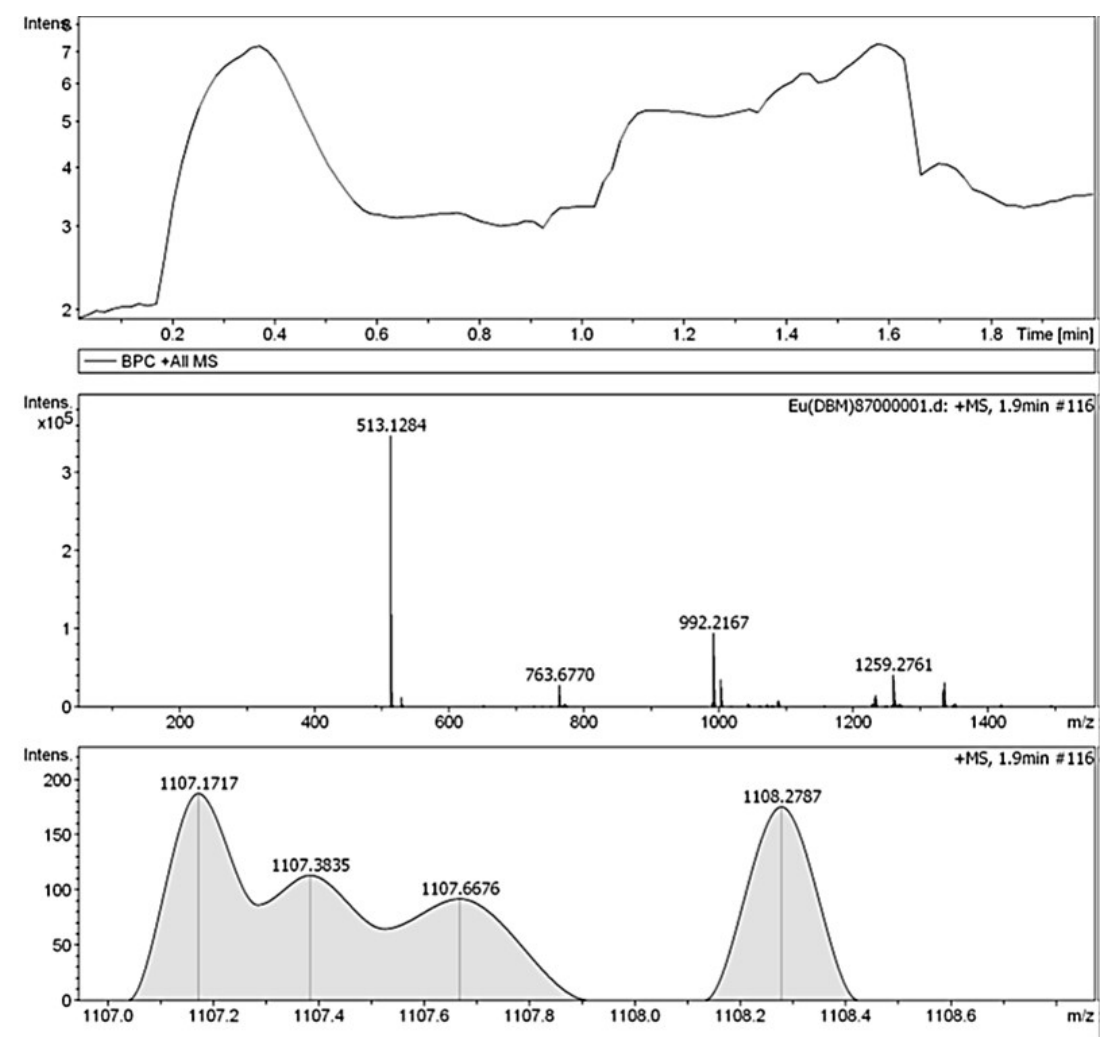


**Fig. S16** Mass spectra of  $\text{Eu}(\text{DDBM})_3\text{L-pCH}_3$



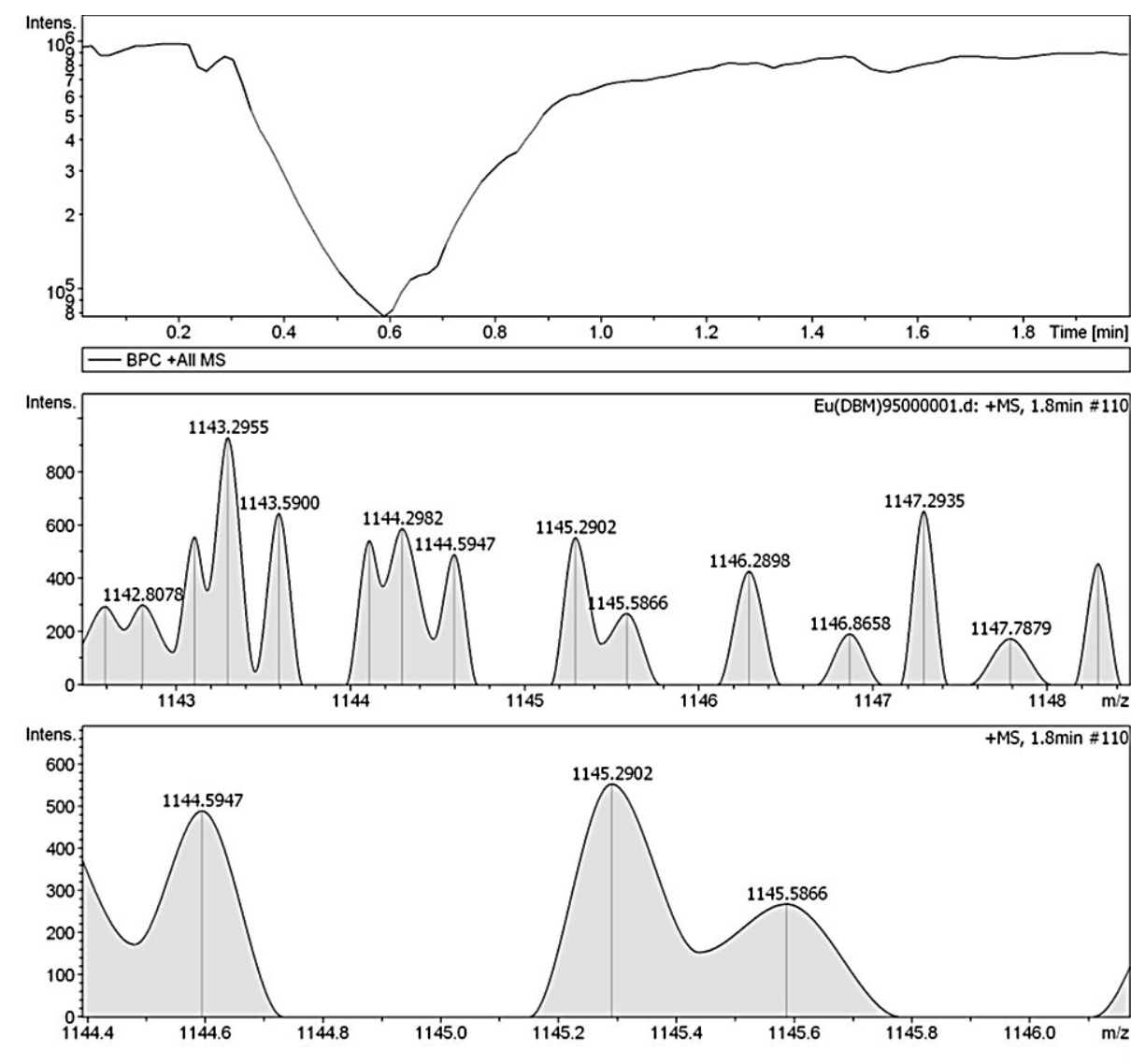


**Fig. S17** Mass spectra of Eu(DDBM)<sub>3</sub>L-Naph-OCH<sub>3</sub>

## Spectroscopic characterization

### Fourier transform-Infrared spectroscopy (FT-IR):

Fig. S9 presents the Fourier transform-Infrared spectra of ligands and their respective Eu(III) complexes. Stretching vibration of all the ligands, as well as Eu(III) complexes, are listed in Table ST1. The Eu(III) complex showed stretching vibration band at ~1600 to belongs to C=N, stretching vibration shift to low frequency from 1632 to 1600 cm<sup>-1</sup> compare to ancillary ligand. The appearance of these bands are

designated the coordination of ancillary ligand with Eu(III) ion in the complex. In the free ancillary ligands, the observed band at  $\sim 1565$ ,  $1598$  and  $852$ ,  $730\text{ cm}^{-1}$ , are assigned to C=C, C=N and C-H stretching and bending vibrations, respectively. In addition, the appeared weak vibration band at  $\sim 520$  and  $\sim 425\text{ cm}^{-1}$  associated with Eu-O and Eu-N. <sup>7, 8</sup> These profoundly confirmed the coordination of DBM and ancillary (N, N) ligand with Eu(III) ion.

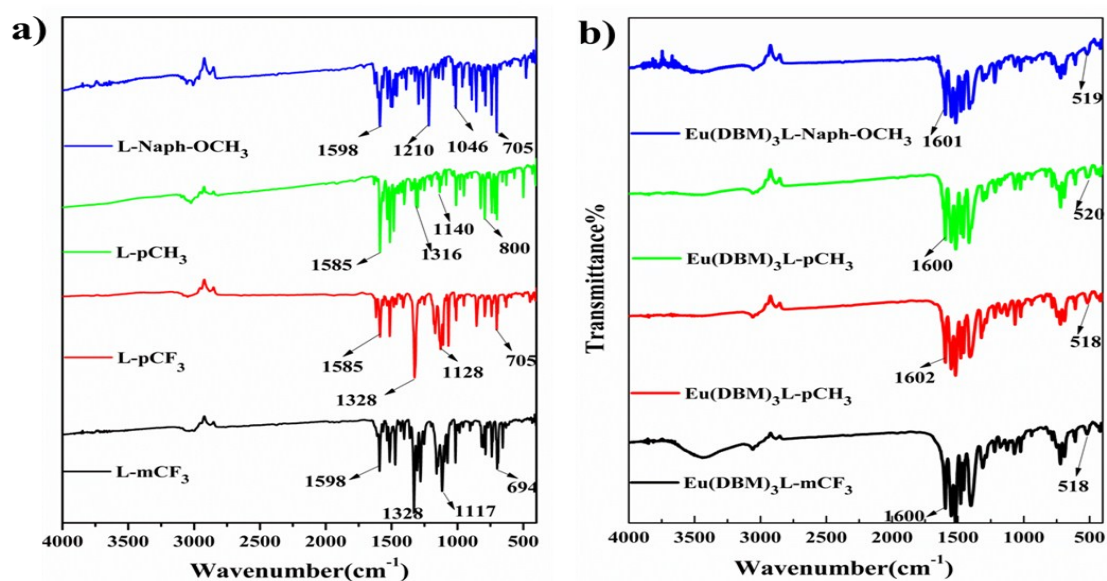


**Fig. S18** FT-IR spectra of the ligands, corresponding Eu(III)-complexes.

**Table ST1.** The Infrared frequencies (wavenumber in  $\text{cm}^{-1}$ ) for free ligand and its corresponding Eu(III)-complexes.

Complex	$\nu(\text{C}=\text{N})$	$\nu(\text{C}-\text{F})$	$\nu(\text{Eu}-\text{O})$	$\nu(\text{Eu}-\text{N})$
$\text{Eu}(\text{DBM})_3\text{L-mCF}_3$	1600	1130	518	428
$\text{Eu}(\text{DBM})_3\text{L-pCF}_3$	1602	1126	518	420
$\text{Eu}(\text{DBM})_3\text{L-pCH}_3$	1600	-	520	425
$\text{Eu}(\text{DBM})_3\text{L-Naph-OCH}_3$	1601	-	519	418
$\text{L-mCF}_3$	1632	1133	-	-

L-pCF <sub>3</sub>	1620	1128	-	-
L-pCH <sub>3</sub>	1630	-	-	-
L-Naph-OCH <sub>3</sub>	1623	-	-	-

**PL and UV spectra:**

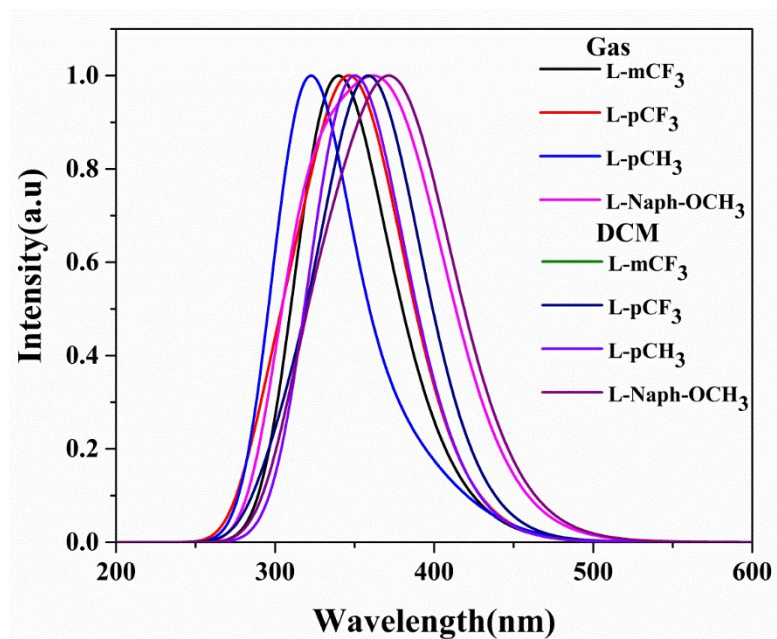


**Fig. S19** Theoretical UV spectra of the ligands in gas phase and DCM solution.

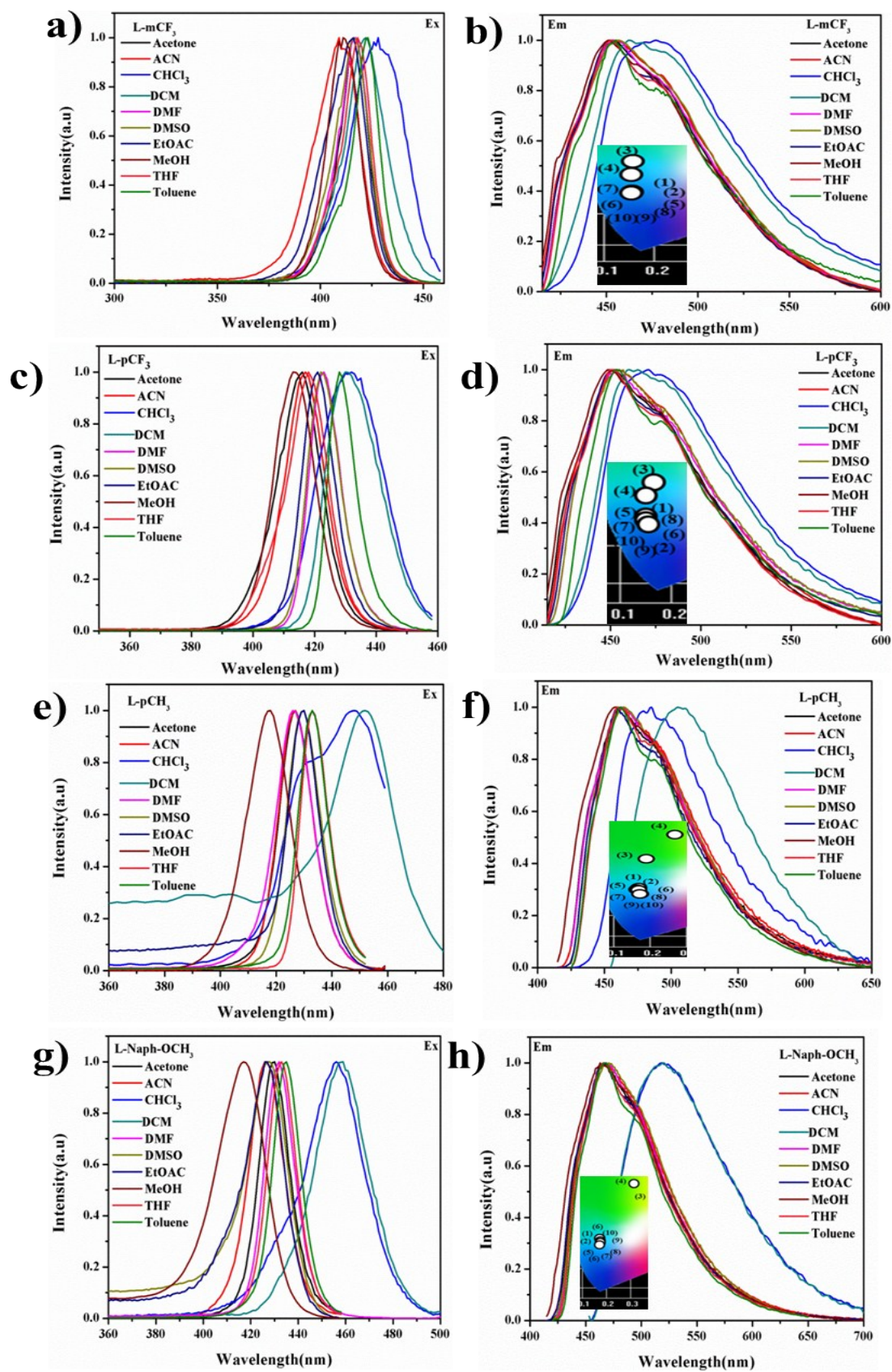
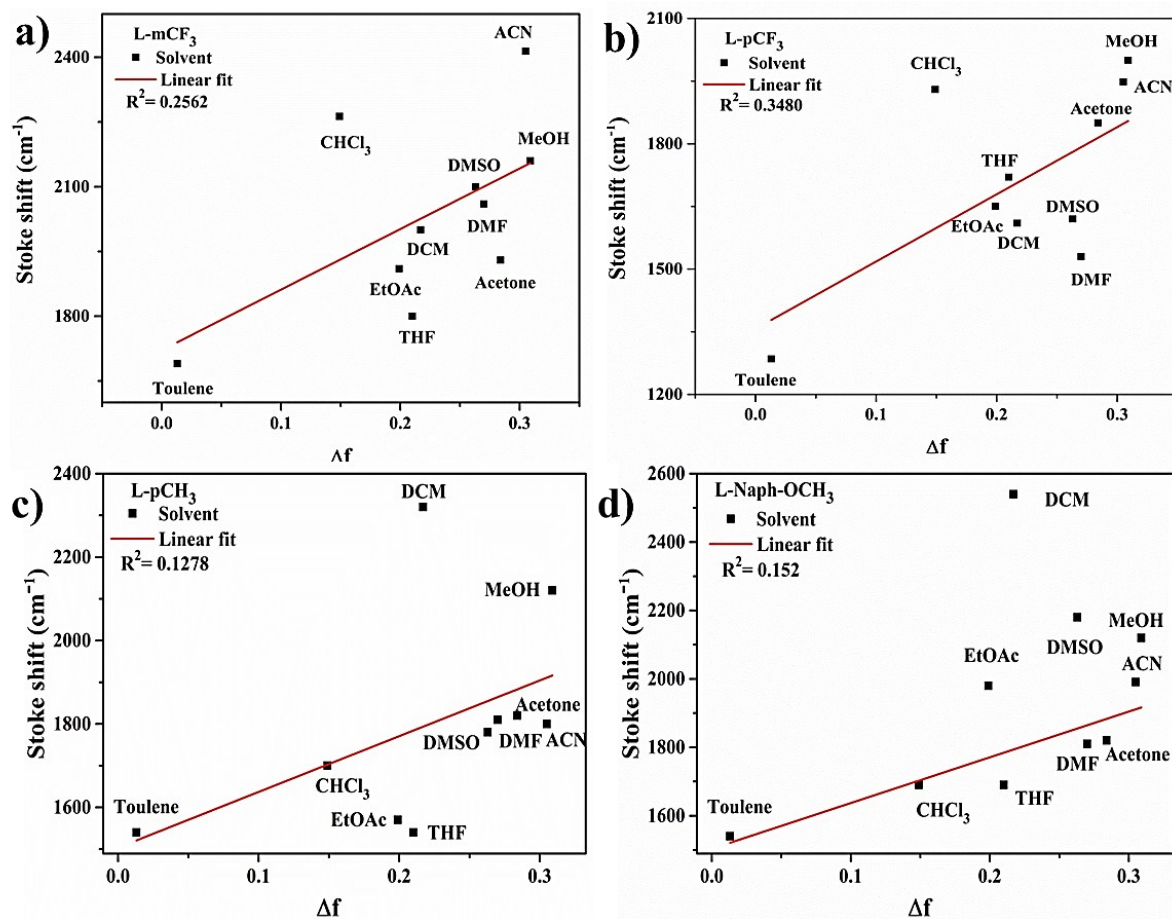


Fig. S20 The solvatochromism PL excitation and emission spectra of all ligands





**Fig. S21** Stokes shift of all ligands  $\Delta\nu$  versus the Lippert solvent parameter  $\Delta f = f(\epsilon) - f(n_2)$ .

The straight line represents the linear fit to the 10 data points.

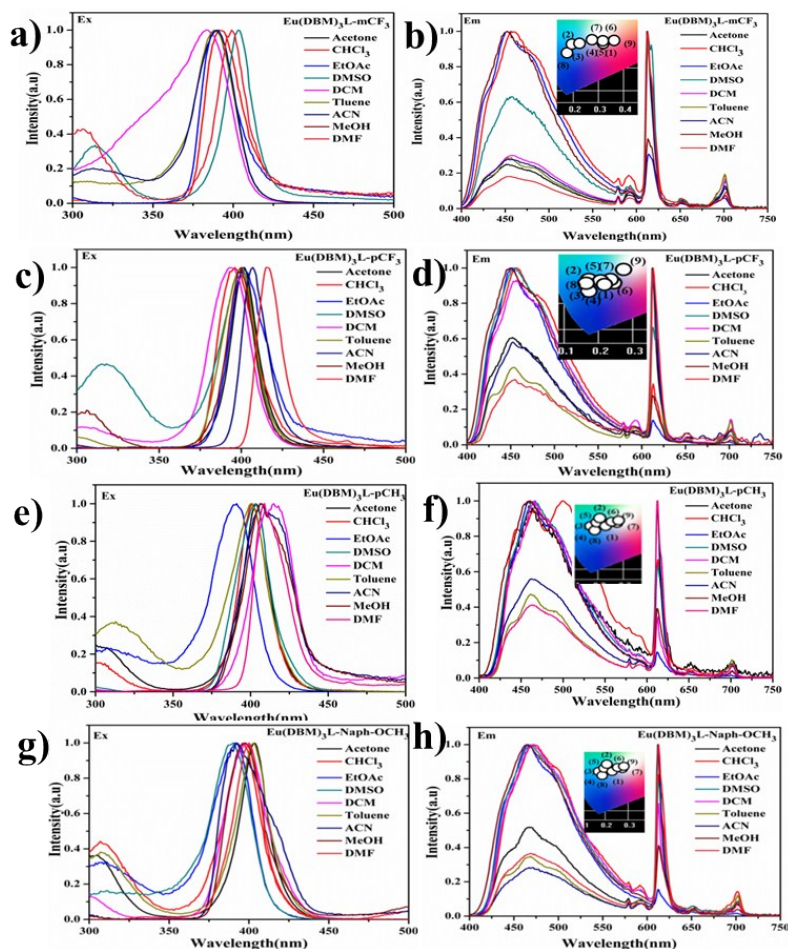


**Fig. S22** The PL emission spectra of the Eu(III) complexes,  $\text{Eu}(\text{DBM})_3\text{L-mCF}_3$ ,  $\text{Eu}(\text{DBM})_3\text{L-pCF}_3$ ,  $\text{Eu}(\text{DBM})_3\text{L-pCH}_3$  and  $\text{Eu}(\text{DBM})_3\text{L-Naph-OCH}_3$  in different solvents and their respective CIE .

**Table ST2.** The calculated CIE from the PL emission data of Eu(III) complexes in different solvents and corresponding asymmetric ratio.

SOLVENT	$\text{Eu}(\text{DBM})_3\text{L-mCF}_3$		$\text{Eu}(\text{DBM})_3\text{L-pCF}_3$		$\text{Eu}(\text{DBM})_3\text{L-pCH}_3$		$\text{Eu}(\text{DBM})_3\text{L-Naph-OCH}_3$	
	(x, y)	AR	(x, y)	AR	(x, y)	AR	(x, y)	AR
DCM	(0.276,0.219)	9.26	(0.201,0.190)	7.18	(0.182,0.232)	2.85	(0.194,0.246)	4.2
DMF	(0.331,0.226)	16.97	(0.278,0.232)	10.15	(0.254,0.227)	9.16	(0.2685,0.248)	13.35
DMSO	(0.233,0.202)	8.39	(0.191,0.175)	6.63	(0.195,0.221)	4.66	(0.202,0.235)	5.39
TOLUENE	(0.289,0.2126)	8.43	(0.243,0.189)	10.09	(0.239,0.221)	10.30	(0.259,0.240)	9.91
MeOH	(0.178,0.161)	4.0	(0.171,0.157)	4.4	(0.179,0.194)	3.86	(0.184,0.215)	3.27
$\text{CHCl}_3$	(0.207,0.205)	5.08	(0.177,0.189)	33.12	(0.209,0.282)	2.82	(0.205,0.253)	4.86
ACN	(0.279,0.215)	9.98	(0.231,0.192)	11.71	(0.226,0.226)	10.83	(0.274,0.251)	13.5
ACETONE	(0.296,0.213)	13.20	(0.221,0.179)	12.73	(0.212,0.230)	6.25	(0.205,0.253)	11.0

**Judd-Ofelt (J –O) analysis:** Among all the lanthanides, Eu(III) ion is most prolific for luminesce properties, due to the presence of magnetic and electric dipole transition present in the spectrum. The MD transition is essential in identifying the nature of crystal field around metal ion, which can be present in the terms of the Judd–Ofelt (J-O) intensity parameters ( $\Omega_2$ ,  $\Omega_4$ , and  $\Omega_6$ ).<sup>2</sup> This can be determined by utilizing the emissions spectra of Eu(III) complex, with the assistance of following eqn 1.

$$\Omega_{\lambda} = \frac{3hc^3A_{o-\lambda}}{4e^2\omega^3\chi < 5D_0 \| U(\lambda) \| ^7 FJ > ^2} \dots\dots\dots(1)$$

The calculated values of  $\Omega_2$  and  $\Omega_4$  intensity parameter of Eu(III) complexes (Eu(DBM)<sub>3</sub>L-mCF<sub>3</sub>, Eu(DBM)<sub>3</sub>L-pCF<sub>3</sub>, Eu(DBM)<sub>3</sub>L-pCH<sub>3</sub> and Eu(DBM)<sub>3</sub>L-Naph-OCH<sub>3</sub>) are compiled in Table ST3. The determined  $\Omega_2$  is a serviceable intensity parameter to comprehend the idea of ligand field around Eu(III) ion. However, the rigidity in a chemical environment can be identified by the help of  $\Omega_4$  (<sup>5</sup>D<sub>0</sub> → <sup>7</sup>F<sub>2</sub>) intensity parameter.

**Table ST3.** Calculated luminescence lifetimes  $\tau_{\text{obs}}$  and intensity parameters of ligands and corresponding Eu(III) complexes.

Compound	Intensity parameters (10 <sup>-20</sup> cm <sup>2</sup> )		A <sub>0-1</sub> in S <sup>-1</sup>	A <sub>0-2</sub> in S <sup>-1</sup>	A <sub>0-4</sub> in S <sup>-1</sup>	Eu-complexes ( $\tau$ / ms / Ligands ( $\tau$ / ns)
	$\Omega_2(10^{-19}$ cm <sup>2</sup> )	$\Omega_4(10^{-20}$ cm <sup>2</sup> )				Toluene
Eu(DBM) <sub>3</sub> L-mCF <sub>3</sub>	1.1472	3.717	50	957.482	147.987	0.213/2.80
Eu(DBM) <sub>3</sub> L-pCF <sub>3</sub>	1.4952	3.832	50	1248.9801	151.883	0.418/2.61

<b>Eu(DBM)<sub>3</sub>L-pCH<sub>3</sub></b>	8.963	2.529	50	749.216	99.941	0.180/3.27
<b>Eu(DBM)<sub>3</sub>L-Naph-OCH<sub>3</sub></b>	1.1724	3.39	50	978.167	133.811	0.153/2.98

### Electrochemical Properties:

The electrochemical properties of the ligands and Eu(III) complex were analysed by cyclic voltammetry. Fig. S23 shows the voltammogram of ligands and Eu(III) complexes and obtained outcomes are tabulated in Table 5. The redox properties of ligand and Eu(III) complex are indispensable as they provide basic information about the highest occupied molecular orbital (HOMO) and lowest unoccupied molecular orbital (LUMO). The HOMO and LUMO levels of all the ligand and Eu(III) complex can be estimated from oxidation potential ( $E_{\text{ox}}(\text{onset})$ ) and the reduction potential ( $E_{\text{red}}(\text{onset})$ ) through equation (2, 3) reported by de Leeuw et al. which is further confirmed by DFT calculation as shown in Fig. 2 (a).

$$\text{HOMO} = [4.4 \text{ V} + E_{\text{ox}}(\text{onset})] \dots \dots \dots (2)$$

$$\text{LUMO} = [4.4 \text{ V} + E_{\text{red}}(\text{onset})] \dots \dots \dots (3)$$

The band gap for ligand and Eu(III) was also calculated by well reported formula HOMO–LUMO. Band gap 3.15, 3.24, 2.89, 2.68 for Eu(III) complexes, Eu(DBM)<sub>3</sub>L-mCF<sub>3</sub>, Eu(DBM)<sub>3</sub>L-pCF<sub>3</sub>, Eu(DBM)<sub>3</sub>L-pCH<sub>3</sub>, Eu(DBM)<sub>3</sub>L-Naph-OCH<sub>3</sub> respectively and the band gap 3.10, 2.83, 3.08, and 2.96 for ligands, L-mCF<sub>3</sub>, L-pCF<sub>3</sub>, L-pCH<sub>3</sub>, L-Naph-OCH<sub>3</sub> respectively. By analysing the obtained result one can conclude that the band gap for ligand and Eu(III) complexes are almost close to each other.



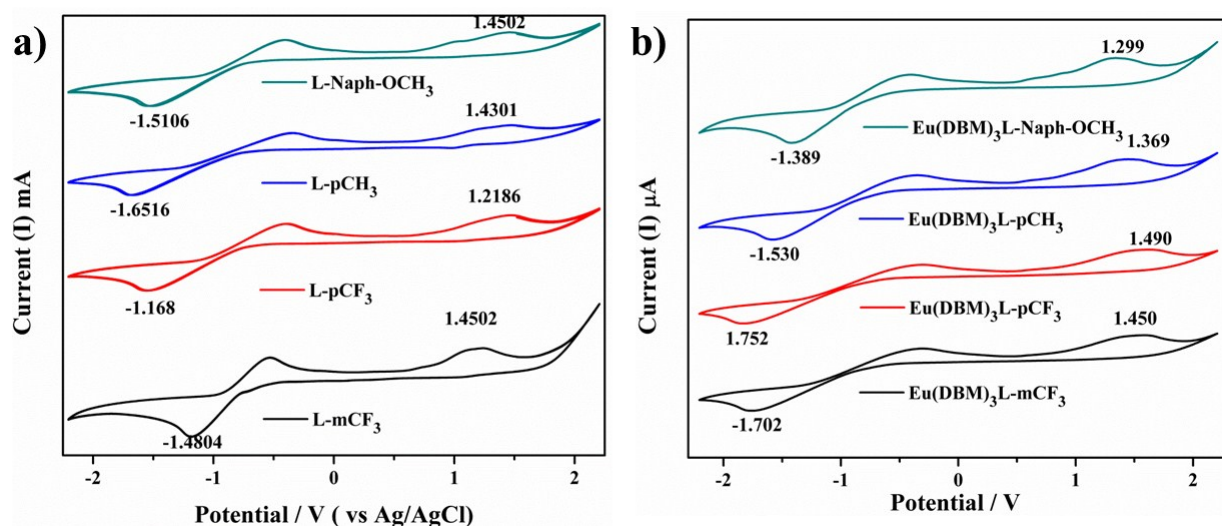


**Fig. S23** Cyclic voltammetry analysis of the ligands and their corresponding complexes.

**Table ST4.** Electrochemical properties of the ligands and respective Eu(III)-complexes.

Compound	$Voltage_{onset}^{Ox}(V)$ $(E_{HOMO} (eV))$	$Voltage_{onset}^{Red}(V)$ $(E_{LUMO} (eV))$	Band gap/ Energy gap $E_g^{Opt} [eV]$	Wavelength(nm)
L-mCF <sub>3</sub>	1.450(-5.850)	-1.48(-2.919)	2.93	423
L-pCF <sub>3</sub>	1.218(-5.618)	-1.168(-2.78)	2.83	438
L-pCH <sub>3</sub>	1.430(-5.830)	-1.651(-2.74)	3.08	402
L-Naph-OCH <sub>3</sub>	1.45(-5.85)	-1.510(-2.88)	2.96	418
Eu(DBM) <sub>3</sub> L-mCF <sub>3</sub>	1.450(-5.85)	-1.702(-2.698)	3.15	393
Eu(DBM) <sub>3</sub> L-pCF <sub>3</sub>	1.490(-5.89)	-1.752(-2.648)	3.24	382
Eu(DBM) <sub>3</sub> L-pCH <sub>3</sub>	1.369(-5.76)	-1.53(-2.87)	2.89	442
Eu(DBM) <sub>3</sub> L-Naph-OCH <sub>3</sub>	1.299(-5.69)	-1.389(-3.01)	2.68	476
$E_{red}^{onset}$ = the onset reduction potentials, $E_{Oxd}^{onset}$ = the onset oxidation potentials, $E_g$ = band gap = $E_{LUMO} - E_{HOMO}$				

## PMMA of ligands:

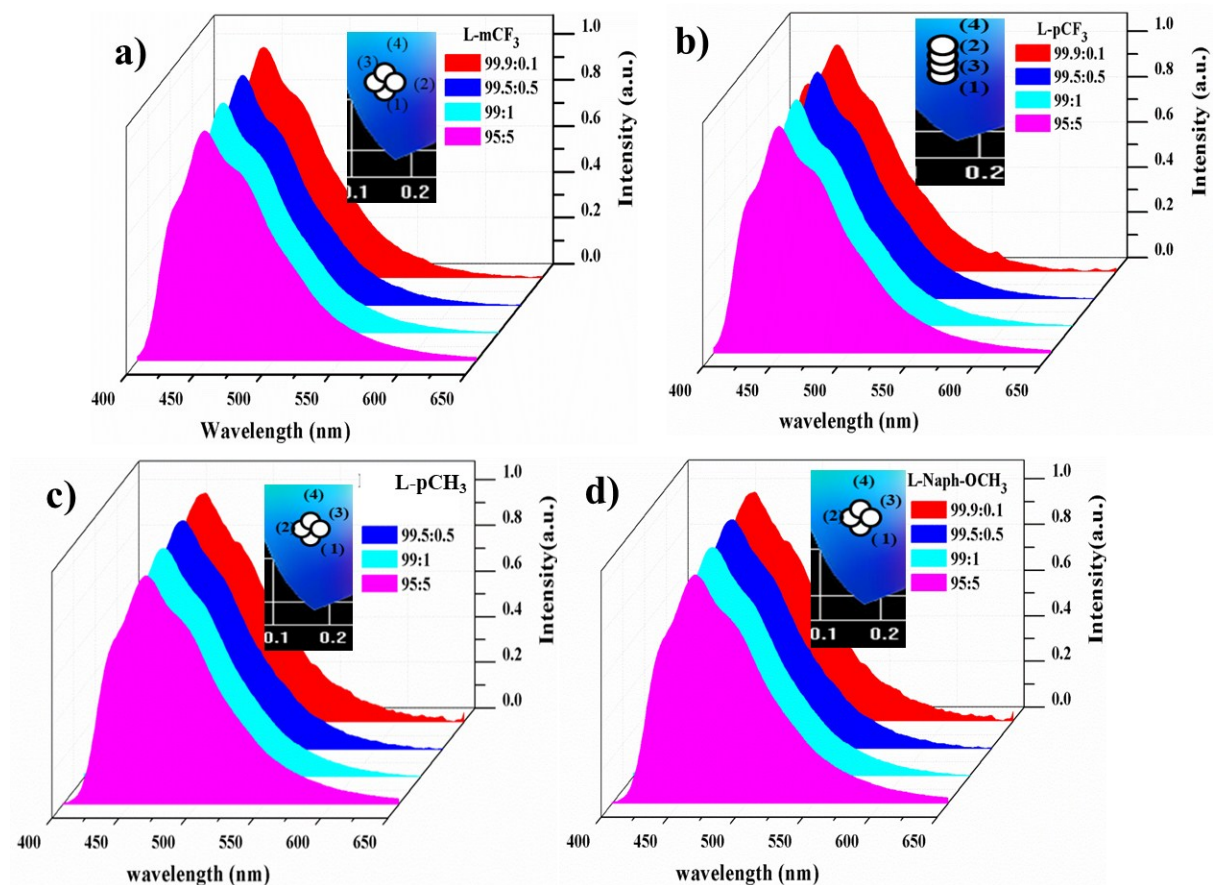


**Fig. S24** PLE spectra of the Eu(III) complexes in solid form (Left) and in solution ( $\text{CHCl}_3$ ) form (Right)

**Table. ST5** Intensity Ratios as Well as CIE Color Coordinates for the Eu(III) Complexes in Different Concentration Ratio Doped PMMA

Characterization	Eu(DBM) <sub>3</sub> L- mCF <sub>3</sub>	Eu(DBM) <sub>3</sub> L- pCF <sub>3</sub>	Eu(DBM) <sub>3</sub> L- pCH <sub>3</sub>	Eu(DBM) <sub>3</sub> L- Naph-OCH <sub>3</sub>
$I_2/I_1$	6.9(1)	2.2(1)	12.8(1)	4.8(1)
(% of Eu <sup>III</sup> )	6.2(2)	12.5(2)	22.3(2)	5.8(2)
	6.4(3)	12.6(3)	13.9(3)	11.2(3)
	12.2(4)	11.7(4)	12.2(4)	13.1(4)

CIE x	0.2379(1%)	0.171(1%)	0.181(1%)	0.261(1%)
	0.2451(2%)	0.2634(2%)	0.305(2%)	0.204(2%)
	0.251(3%)	0.268(3%)	0.335(3%)	0.364(3%)
	0.3628(4%)	0.301(4%)	0.335(4%)	0.401(4%)
y	0.1840(1%)	0.1435(1%)	0.177(1%)	0.227(1%)
	0.1897(2%)	0.1743(2%)	0.221(2%)	0.185 (2%)
	0.1906(3%)	0.178(3%)	0.223(3%)	0.240(3%)
	0.22947(4%)	0.191(4%)	0.221(4%)	0.257(4%)

### Phosphorescence study at 77K

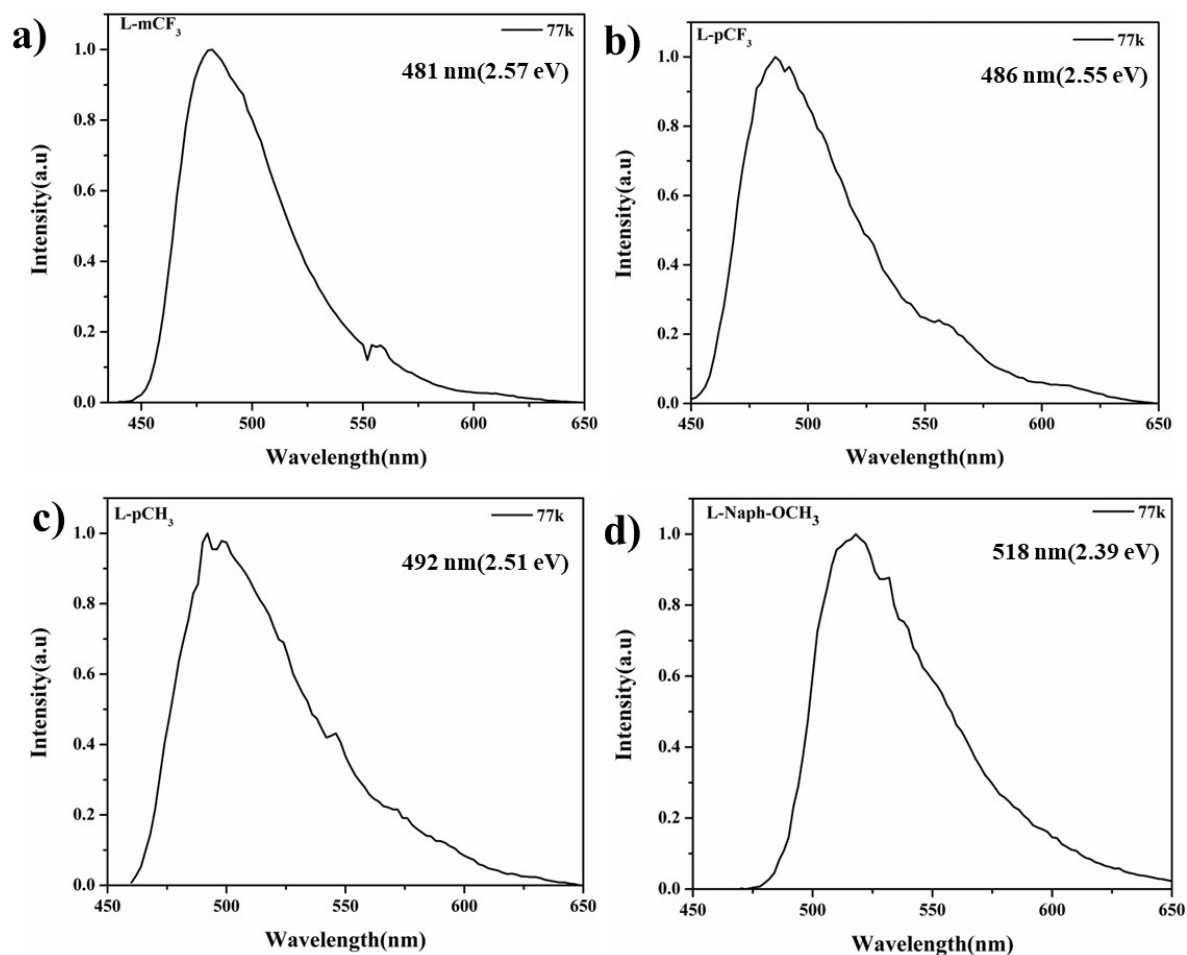


**Fig. S25** Phosphorescence emission spectrum of ligands, L-mCF<sub>3</sub>, L-pCF<sub>3</sub>, L-pCH<sub>3</sub> and L-Naph-OCH<sub>3</sub> at 77 K.

**Table ST6. CIE Color Coordinates for the Eu(III) Complexes in Different Concentration Ratio coated with LED**

CIE	Eu(DBM) <sub>3</sub> L-mCF <sub>3</sub>	Eu(DBM) <sub>3</sub> L-pCF <sub>3</sub>	Eu(DBM) <sub>3</sub> L-pCH <sub>3</sub>	Eu(DBM) <sub>3</sub> L-Naph-OCH <sub>3</sub>
<b>1:10 (x, y)</b>	(0.354, 0.278)	(0.313, 0.322)	(0.280, 0.330)	(0.257, 0.091)
<b>1:50 (x, y)</b>	(0.401, 0.309)	(0.360, 0.310)	(0.334, 0.333)	(0.405, 0.209)

### Thermal Study:

The thermal stability of ligand and Eu(III) complex paramount importance for the optical properties and device performance. The thermal stability of Eu(III) complexes (Eu(DBM)<sub>3</sub>L-mCF<sub>3</sub>, Eu(DBM)<sub>3</sub>L-pCF<sub>3</sub>, Eu(DBM)<sub>3</sub>L-pCH<sub>3</sub>, Eu(DBM)<sub>3</sub>L-Naph-OCH<sub>3</sub>) is calculated by TGA analyses within the range from ambient temperature to 1000°C at a heating rate of 10°C/min under the nitrogen atmosphere. The related evidence is shown in Fig. S26. All ligands and Eu(III) complexes exhibited great thermal stability with good thermal decomposition temperature (Td) in the range 463–478 °C and 222 - 329°C, respectively which indicate that these are potential candidate for device fabrication. Their amazing thermal stability is fortified from the three step disintegration pathway with T<sub>d</sub> at 5% weight loss over 400°C. In the first step, there is some weight loss at 100–115°C is due to the volatilization of water molecules present in complexes (minor decomposition). In the second step the decomposition was observed due the presence of DBM anionic ligand in the Eu(III) complexes. Decomposition of ancillary ligand from the Eu(III) complexes are the major thermal decomposition.

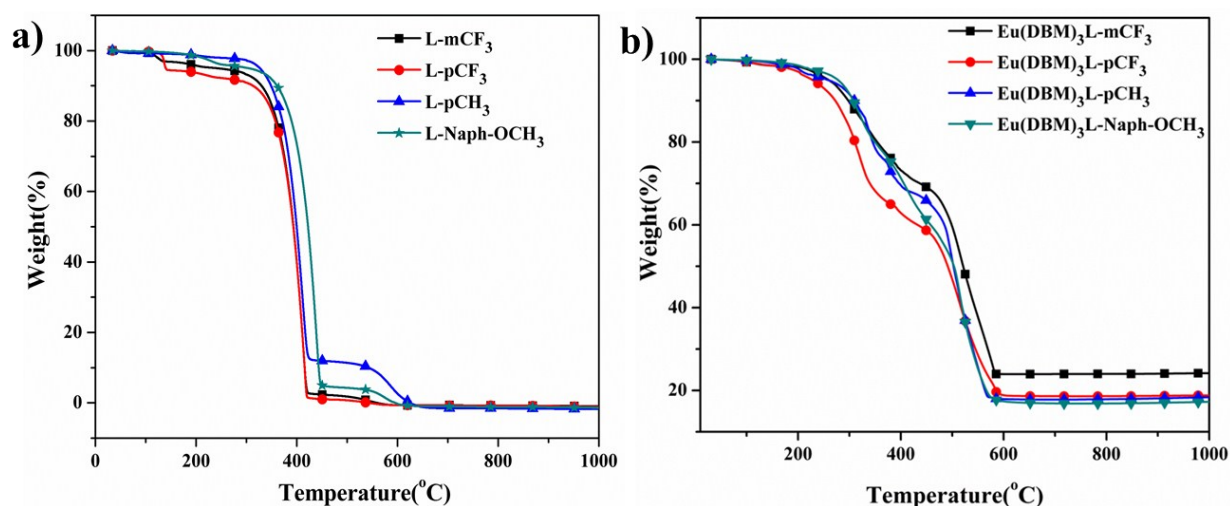


**Fig. S26** TG curve of ligands and their respective Eu(III) complexes recorded under N<sub>2</sub> atmosphere.

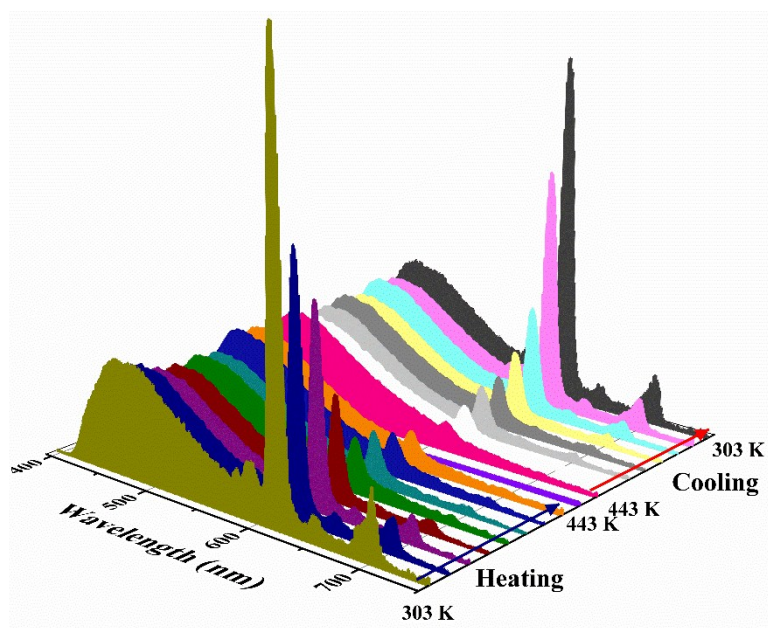


**Fig. 27.** Temperature dependent PL study during heating and cooling for the complex  
Eu(DBM)<sub>3</sub>L-mCF<sub>3</sub>

#### DFT Analysis:

**Table ST7.** The computed vertical transitions and their oscillator strengths (*f*) and configuration of the ligands.

Luminophores	State	Energy (eV)	$\lambda_{\text{max}}$ nm	<i>f</i>	Configuration
<b>L-mCF<sub>3</sub></b>	Gas	3.327	372.6	0.092	HOMO→LUMO (67.37%)

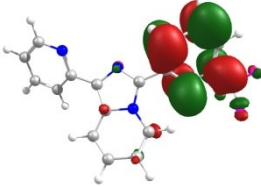
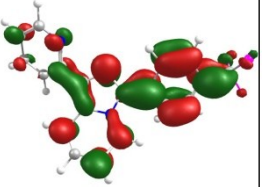
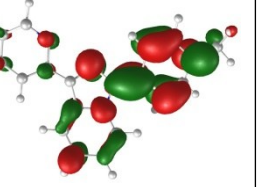
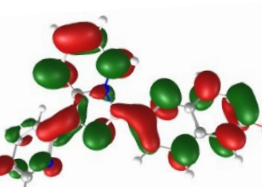
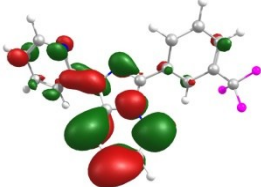
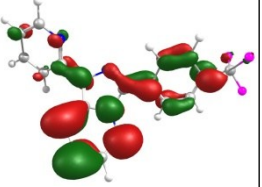
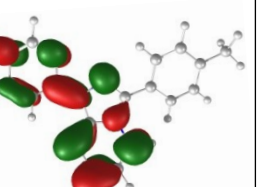
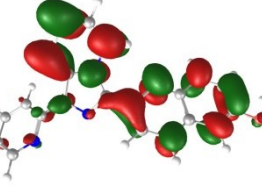
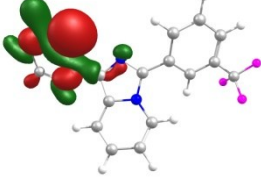
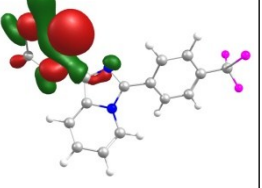
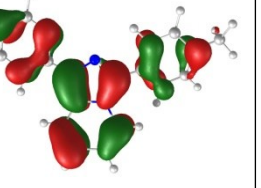
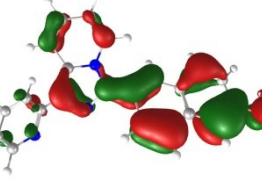
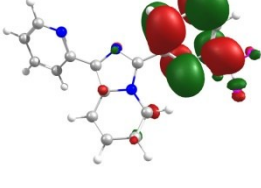
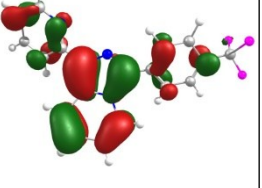
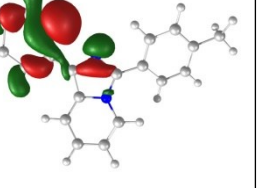
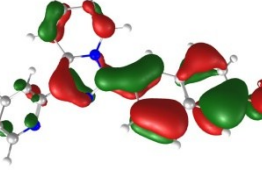
Singlet				7	HOMO→LUMO+1 (20.12%)
		3.683	336.6	0.367 0	HOMO→LUMO (12.53%) HOMO→LUMO+1 (68.33%)
		3.821	324.4	0.018	HOMO→LUMO+2 (69.71%)
	DCM	3.394	365.29	0.206	HOMO→LUMO (67.65%)
		3.589	345.37	0.446	HOMO→LUMO (10.95%) HOMO→LUMO+1 (68.96%)
		3.793	326.81	0.028	HOMO→LUMO+2 (70.04%)
Triplet	Gas	2.336	530.7	0	HOMO→LUMO (67.97%)
		2.857	433.8	0	HOMO-4→LUMO+2 (10.15%) HOMO→LUMO+1 (64.40%) HOMO→LUMO+3 (14.43%)
		3.260	380.2	0	HOMO→LUMO (36.36%) HOMO→LUMO+1 (30.84%) HOMO→LUMO+3 (44.54%) HOMO→LUMO+4 (13.18%)
	DCM	2.403	516.32	0	HOMO-3→LUMO (10.38%) HOMO→LUMO (67.39%)
		2.840	436.4	0	HOMO-4→LUMO+2 (11.48%) HOMO→LUMO+1 (64.84%) HOMO→LUMO+3 (12.68%)
		3.257	380.5	0	HOMO→LUMO+3 (54.10%) HOMO→LUMO+4 (31.04%)
<b>L-pCF<sub>3</sub></b> Singlet	Gas	3.315	373.9	0.085	HOMO→LUMO (62.28%) HOMO→LUMO+1 (27.92%) HOMO→LUMO+1 (15.13%)
		3.562	348.0	0.426	HOMO→LUMO+1 (63.93%)
		4.047	306.3	0.182 3	HOMO→LUMO+2 (65.76%)
	DCM	3.399	364.6	0.215	HOMO→LUMO (17.15%) HOMO→LUMO+1 (66.58%)
		3.442	360.12	0.501	HOMO→LUMO (67.68%)
		3.954	313.57	0.183	HOMO→LUMO+1 (10.12%) HOMO→LUMO+2 (68.36%)
Triplet	Gas	2.329	532.1	0	HOMO→LUMO (65.62%) HOMO→LUMO+1 (17.72%)
		2.776	446.5	0	HOMO-2→LUMO+1 (11.86%) HOMO→LUMO+1 (63.57%) HOMO→LUMO+2 (12.43%)
		3.258	380.4	0	HOMO→LUMO+2 (59.29%) HOMO→LUMO+4 (21.90%)
	DCM	2.405	515.3	0	HOMO→LUMO (35.13%) HOMO→LUMO+1 (57.57%)
		2.742	452.1	0	HOMO→LUMO (56.89%) HOMO→LUMO+2 (10.12%)
		3.261	380.0	0	HOMO-3→LUMO+1 (11.71%) HOMO→LUMO+1 (12.41%)

					HOMO→LUMO+2 (55.05%)
<b>L-pCH<sub>3</sub></b> Singlet	Gas	3.2517	381.2	0.093	HOMO→LUMO (67.65%)
		3.815	324.9	0.404	HOMO→LUMO+1 (65.95%)
		3.952	313.5	0.238	HOMO→LUMO (16.02%) HOMO→LUMO+1 (20.85%) HOMO→LUMO+2 (62.13%)
	DCM	3.317	373.70	0.200 3	HOMO→LUMO (68.40%)
		3.731	332.23	0.473 7	HOMO→LUMO+1 (66.49%)
		3.884	319.21	0.221	HOMO→LUMO (13.76%) HOMO→LUMO+1 (22.16%) HOMO→LUMO+2 (64.30%)
Triplet	Gas	2.290	541.3	0	HOMO-4→LUMO (10.21%) HOMO→LUMO (67.75%)
		2.936	423.7	0	HOMO-3→LUMO+4 (11.49%) HOMO→LUMO+1 (61.54%) HOMO→LUMO+2 (24.69%)
		3.212	386	0	HOMO→LUMO+2 (55.21%) HOMO→LUMO+3 (24.32%)
	DCM	2.352	526.9	0	HOMO→LUMO (66.91%)
		2.931	422.9	0	HOMO→LUMO+1 (60.75%) HOMO→LUMO+2 (25.86%)
		3.201	387.2	0	HOMO-4→LUMO (14.19%) HOMO-1→LUMO+2 (10.31%) HOMO→LUMO (11.59%) HOMO→LUMO+2 (50.90%) HOMO→LUMO+3 (31.95%)
<b>L-Naph-OCH<sub>3</sub></b> Singlet	Gas	3.168	391.2	0.051	HOMO→LUMO (58.61%) HOMO→LUMO+2 (14.71%)
		3.317	373.7	0.312	HOMO→LUMO (35.48%) HOMO→LUMO+1 (59.50%)
		3.838	322.9	0.285	HOMO→LUMO+2 (48.4%) HOMO→LUMO+3 (47.8%)
	DCM	3.235	383.2	0.086 7	HOMO→LUMO (57.25%) HOMO→LUMO+3 (11.09%)
		3.270	379.11	0.487 8	HOMO→LUMO (39.56%) HOMO→LUMO+1 (57.17%)
		3.756	330.09	0.289 5	HOMO→LUMO+2 (68.3%)
Triplet	Gas	2.253	550.1	0	HOMO→LUMO (60.38%)
		2.448	506.4	0	HOMO→LUMO (18.53%) HOMO→LUMO+1 (54.5%)
		3.061	405	0	HOMO-1→LUMO+2 (10.72%) HOMO→LUMO+2 (37.57%) HOMO→LUMO+4 (11.11%) HOMO→LUMO+5 (11.77%)



	DCM	2.321	534.0	0	HOMO→LUMO+1 (46.46%)
		2.447	506.5	0	HOMO-1→LUMO (32.65%) HOMO→LUMO (39.85%) HOMO→LUMO+1 (42.99%)
		3.092	400.9	0	HOMO-1→LUMO (36.77%) HOMO-1→LUMO+1 (10.39%) HOMO→LUMO+3 (46.26%) HOMO→LUMO+4 (15.55%) HOMO→LUMO+5 (12.43%)

**Table ST8.** The HOMO-LUMO and HOMO-1, LUMO+1 energy levels of the ligand.

	L-mCF <sub>3</sub>	L-pCF <sub>3</sub>	L-pCH <sub>3</sub>	L-Naph-OCH <sub>3</sub>
LUMO+1				
LUMO				
HOMO				
HOMO-1				

**Table ST9.** Cartesian coordinates for optimized geometry of L-MCF<sub>3</sub>

6	-1.383975	-0.963676	0.186793
6	-0.551251	0.168887	0.346307
6	-1.102152	1.398633	0.579095



6	-2.517880	1.533943	0.684938
6	-3.329202	0.453774	0.543311
6	-3.348502	-2.045631	0.148829
6	-1.201338	-2.343178	0.024372
1	0.521223	0.035047	0.304644
1	-0.469567	2.267883	0.706922
1	-2.964613	2.495839	0.899190
1	-4.400503	0.495983	0.659181
6	1.228898	-5.014202	0.314923
6	2.375652	-4.547970	-0.325982
6	2.330271	-3.281427	-0.899625
6	1.157888	-2.542313	-0.802737
6	0.060203	-3.086844	-0.117145
1	1.218307	-6.003422	0.765924
1	3.265966	-5.162953	-0.378841
1	3.187838	-2.880991	-1.429037
1	1.078663	-1.573847	-1.280792
7	-2.407418	-2.965588	0.023335
7	0.101099	-4.314688	0.427734
7	-2.780917	-0.785870	0.270754
6	-6.523207	-3.961535	0.680226
6	-5.184252	-3.602152	0.668493
6	-4.780481	-2.354478	0.158596
6	-5.756542	-1.499732	-0.363760
6	-7.103245	-1.865369	-0.338513
6	-7.496511	-3.091602	0.186792
1	-6.817452	-4.924625	1.080509
1	-4.422878	-4.274436	1.042602
1	-5.479161	-0.564655	-0.832501
1	-8.543078	-3.364890	0.202639
6	-8.109955	-0.902115	-0.903351
9	-7.866810	-0.626328	-2.206081

9	-8.079504	0.288154	-0.253098
9	-9.373455	-1.363737	-0.823536

**Table ST10. Cartesian coordinates for optimized geometry of L-pCF<sub>3</sub>**

6	-2.304182	1.269065	-0.130974
6	-3.229683	2.327640	-0.285992
6	-2.784503	3.609848	-0.453545
6	-1.383995	3.874992	-0.496511
6	-0.484292	2.866674	-0.358107
6	-0.251740	0.366452	-0.048333
6	-2.366636	-0.126828	-0.023166
1	-4.286322	2.096992	-0.293402
1	-3.488245	4.423058	-0.578137
1	-1.018958	4.880196	-0.661171
1	0.582390	3.006538	-0.430173
6	-4.524922	-2.999430	-0.484837
6	-5.733911	-2.660530	0.120915
6	-5.829467	-1.412574	0.728066
6	-4.728569	-0.565649	0.698200
6	-3.559268	-0.985961	0.044573
1	-4.404421	-3.969556	-0.960578
1	-6.563919	-3.356739	0.121807
1	-6.740468	-1.108788	1.231853
1	-4.758949	0.391102	1.204582
7	-1.110379	-0.638011	0.005847
7	-3.464296	-2.195396	-0.533513
7	-0.927274	1.574141	-0.149812
6	3.093725	-1.247727	-0.502787
6	1.730951	-1.002552	-0.536877
6	1.200760	0.186003	-0.004324
6	2.080607	1.104107	0.588146

6	3.449282	0.858220	0.620812
6	3.961457	-0.312120	0.067773
1	3.490154	-2.160777	-0.929785
1	1.049608	-1.723403	-0.969486
1	1.702467	1.997048	1.069019
1	4.1172720	1.573754	1.082641
6	5.432673	-0.607684	0.131566
9	6.170773	0.505398	0.336329
9	5.882025	-1.182293	-1.007037
9	5.732003	-1.464339	1.137278

**Table ST11. Cartesian coordinates for optimized geometry of L-pCH<sub>3</sub>**

6	-1.212145	1.292938	-0.122805
6	-1.979820	2.469689	-0.293610
6	-1.359545	3.675069	-0.472703
6	0.065440	3.742330	-0.511373
6	0.814815	2.620225	-0.356604
6	0.699469	0.118209	-0.016187
6	-1.464722	-0.078486	-0.001039
1	-3.058436	2.389667	-0.303801
1	-1.942760	4.577043	-0.609126
1	0.567315	4.685212	-0.684738
1	1.891349	2.606384	-0.420277
6	-3.997509	-2.628911	-0.460684
6	-5.156492	-2.114532	0.118263
6	-5.083311	-0.857314	0.709797
6	-3.873383	-0.175464	0.690517
6	-2.763998	-0.764136	0.061066
1	-4.007677	-3.613341	-0.922418
1	-6.076860	-2.686046	0.111594
1	-5.949998	-0.420792	1.194124
1	-3.776037	0.7824530	1.186052

7	-0.288006	-0.757846	0.044670
7	-2.833064	-1.983864	-0.500219
7	0.194906	1.404816	-0.137110
6	3.826890	-1.894444	-0.473779
6	2.504708	-1.480512	-0.520148
6	2.118610	-0.247128	0.030784
6	3.102267	0.534930	0.650360
6	4.428709	0.110914	0.688156
6	4.818992	-1.103809	0.122303
1	4.097929	-2.851240	-0.909266
1	1.744074	-2.104788	-0.971827
1	2.835124	1.458515	1.149718
1	5.168995	0.732283	1.181748
6	6.257525	-1.558345	0.148043
1	6.871868	-0.903172	0.768842
1	6.345599	-2.575364	0.541116
1	6.688430	-1.563057	-0.858736

**Table ST12: Cartesian coordinates for optimized geometry of L-Naph-OCH<sub>3</sub>**

**L-Naph-OCH<sub>3</sub>**

6	-2.672805	1.264119	0.148684
6	-3.487352	2.415815	0.259382
6	-2.920022	3.640819	0.477508
6	-1.504717	3.752616	0.619538
6	-0.711169	2.654411	0.522999
6	-0.723095	0.148394	0.184982
6	-2.874263	-0.115013	0.015877
1	-4.560817	2.301279	0.192713
1	-3.539644	4.524162	0.567317
1	-1.046417	4.710753	0.826648
1	0.357131	2.674678	0.667462
6	-5.354880	-2.741550	0.299035

6	-6.481996	-2.265631	-0.368920
6	-6.403675	-1.008183	-0.959317
6	-5.220767	-0.288269	-0.851566
6	-4.144313	-0.840380	-0.137713
1	-5.369274	-3.724395	0.763964
1	-7.381795	-2.866010	-0.429315
1	-7.244325	-0.600571	-1.510140
1	-5.116203	0.670898	-1.343164
7	-1.678144	-0.757596	0.059612
7	-4.217505	-2.059941	0.423245
7	-1.274499	1.4195420	0.263700
6	2.368893	-1.8463020	0.848520
6	1.062653	-1.448765	0.784428
6	0.703048	-0.180947	0.233472
6	1.702954	0.630789	-0.268514
6	3.066639	0.245561	-0.213758
6	3.418682	-1.015861	0.362813
1	2.621413	-2.811386	1.274821
1	0.266479	-2.088701	1.142471
1	1.464036	1.566574	-0.760441
6	4.104903	1.062172	-0.721158
6	5.423197	0.672306	-0.66010
6	4.774099	-1.397371	0.419619
6	5.765672	-0.574166	-0.079506
8	7.045294	-1.036191	0.023563
6	8.107140	-0.244503	-0.489697
1	9.016428	-0.81268	-0.300389
1	8.004557	-0.080249	-1.568185
1	8.175533	0.722311	0.021489
1	6.189754	1.323385	-1.058061
1	3.851331	2.018041	-1.168106
1	5.058011	-2.348763	0.854120

## Reference:

1. X. Zhou, X. Zhao, Y. Wang, B. Wu, J Shen,. L. Li and Q. Li, *Inorg. Chem.*, 2014, **53**, 12275-12282.
- 2 B. Rajamouli, P. Sood, S. Giri, V. Krishnan and V. Sivakumar, *Eur. J. Inorg. Chem.* **2016**, 3900-3911.
3. B. Rajamouli and V. Sivakumar, *New J. Chem.*, 2017, **41**, 1017-1027.
4. K. Singh, R. Boddula and V. Sivakumar, *Inorg. Chem.*, 2017, **56 (15)**, 9376-9390.
5. K. Qiu, Y. Liu, H. Huang, C. Liu, H. Zhu, Y. Chen, L. Ji and H. Chao, *Dalton Trans.*, 2016, **45**, 16144-16147
6. B. Rajamouli, S., Kasturi, G. Santanab and V. Sivakumar, *Inorg. Chem.*, 2017, **56, 17**, 10127-10130.
7. Z. A. Taha, A. M. Ajlouni, K. A. Al-Hassan, A. K. Hijazi and A. B. Faiq, *Spectrochim. Acta, Part A*, 2011, **81**, 317–323.
8. S. Chen, R.-Q. Fan, S. Gao, X.-M. Wang and Y.-L. Yang, *J. Lumin.*, 2014, **149**, 75-85.